

Working Report 2013-24

Ion-Selective Electrodes in Porewater Chemistry Measurement of Compacted Bentonite

**Arto Muurinen
Joonas Järvinen
VTT**

August 2013

Working Reports contain information on work in progress
or pending completion.

The conclusions and viewpoints presented in the report
are those of author(s) and do not necessarily
coincide with those of Posiva.

ABSTRACT

The aim of this study was to develop and test Ion-Selective Electrodes (ISE) for measuring the chemical conditions in the porewater of compacted bentonite. Ion-selective electrodes are sensors that convert the chemical activity of an ion in a solution into an electrical potential. The high swelling pressure and low content of free water in the compacted bentonite together with the measurement times of at least a few weeks set special requirements on the mechanical strength and potential stability of the electrodes. The focus of this study was directed to the electrodes of precipitate-type membranes. From the literature, promising electrode types were found for chloride, sulphate, sodium and calcium. The chloride electrode was prepared from the commercial Ag-AgCl pellet prepared from a fine-grain homogeneous mixture of silver and silver chloride. The membrane pellet for the sulphate electrode was prepared from a four-component mixture of PbSO_4 , PbS , Ag_2S and Cu_2S pressed overnight at 7 000 bar at 150 °C. A Natrium Super Ionic Conductor (Nasicon) pellet was used for the membrane of the sodium electrode. The Nasicon powder was pressed for two hours at 4 000 bar at 200 °C and sintered in an oven at 1 000 °C. A europium-doped LaF_3 pellet coated with colloidal CaF_2 and heated to 400 °C was used for the membrane of the calcium electrode. The sulphate, sodium and calcium membranes were fixed with epoxy to the electrode body and the electric contact between the membrane and the electric wire in the electrode was made with silver epoxy. The leak-free electrode LF-2 of Innovative Instruments, Inc., Tampa, USA, was used as the reference electrode. The electrode is based on the Ag/AgCl wire in 3.4 M KCl solution and uses a leak-free conductive junction. The electrode body is constructed from PEEK.

The calcium and chloride electrodes were tested together in purified calcium bentonite where CaCl_2 solution was added as the porewater. The sodium and sulphate electrodes were tested together in purified sodium bentonite where Na_2SO_4 solution was added as the porewater. The calibration of the electrodes was done in CaCl_2 and Na_2SO_4 solutions before and after the measurement in the bentonite. Mechanically all the electrodes were strong enough for the measurement in the compacted bentonite of a dry density of up to 1.66 g/cm^3 but the potential stability was a problem except for the chloride electrode. Its calibration curves before and after the experiments were close to each other. The chloride concentrations measured in the bentonite with the ISE were clearly higher than the concentrations obtained assuming a homogeneous distribution of chloride in the porewater. The chloride porosities evaluated on the basis of the ISE measurements were in line with the chloride porosities determined earlier in exclusion experiments. The probable explanation is that chloride was owing to its negative charge excluded from the small interlamellar pores and was in the larger, non-interlamellar pores where the ISEs measure the concentration. The potentials of the calcium, sulphate and sodium electrodes stabilized much more slowly than the chloride electrodes, the calibration curves before and after the experiment were in many cases far from each other, and the obtained results were unreliable.

Keywords: Bentonite, porewater, ion-selective electrode.

Ioniselektiiviset elektrodit kompaktoidun bentoniitin huokosvesikemian mittauksissa

TIIVISTELMÄ

Tämän tutkimuksen tarkoituksena oli kehittää ja testata ioniselektiivisiä elektrodeja kemiallisten olosuhteiden mittaamiseen puristetun bentoniitin huokosvedessä. Ioniselektiiviset elektrodit ovat sensoreita, jotka muuntavat liuoksessa olevan ionin kemiallisen aktiivisuuden sähköiseksi potentiaaliksi. Puristetun bentoniitin suuri paisuntapaine ja alhainen vapaan veden pitoisuus sekä ainakin muutaman viikon pituinen mittausaika asettavat erityisiä vaatimuksia elektrodien mekaaniselle lujuudelle ja potentiaalilin stabiilisuudelle. Tässä tutkimuksessa keskityttiin sakkamembraaneihin perustuviin elektrodeihin. Kirjallisuudesta löytyi lupaavia elektrodityyppejä kloridille, sulfaatile, natriumille ja kalsiumille. Kloridielektrodi valmistettiin kaupallisesta Ag-AgCl-pelletistä, joka oli valmistettu hopean ja hopeakloridin homogeenisesta seoksesta. Sulfaattielektrodin membraanipelletti valmistettiin neljän komponentin (PbSO₄, PbS, Ag₂S and Cu₂S) seoksesta jota puristettiin yli yön 7000 barin paineessa ja 150 °C lämpötilassa. Nasion-pellettiä (Natrium Super Ionic Conductor) käytettiin natriumelektrodin membraanina. Nasion-pulveria puristettiin kaksi tuntia 4000 barissa 200 °C lämpötilassa ja sintrattiin sen jälkeen uunissa 1000 °C:n lämpötilassa. Kalsiumelektrodin membraani valmistettiin CaF₂-kolloidilla pinnotetusta, europiumilla seostetusta LaF₃ pelletistä, joka kuumennettiin 400 °C:n lämpötilaan. Sulfaatti-, natrium- ja kalsiummembraanit kiinnitettiin epoksilla elektrodirunkoon ja sähköinen kontakti membraanin ja elektrodin sähköjohtimen välille tehtiin hopeaepoksilla. Vuotamatonta LF-2 elektrodia (Innovative Instruments, Inc., Tampa, USA) käytettiin referenssielektrodina. Elektrodi perustuu Ag/AgCl-elektrodiin 3.4 M KCl-liuoksessa ja vuotamatomaan, johtavaan rajapintaan.

Kalsium- ja kloridielektrodit testattiin yhdessä puhdistetussa kalsiumbentoniitissa, johon CaCl₂-liuosta oli lisätty huokosvedeksi. Natrium- ja sulfaattielektrodit testattiin yhdessä puhdistetussa natriumbentoniitissa johon Na₂SO₄ liuosta oli lisätty huokosvedeksi. Elektrodien kalibrointi tehtiin CaCl₂- ja Na₂SO₄-liuoksissa ennen ja jälkeen bentoniittimittausta. Pitoisuudet huokosvedessä laskettiin mitatusta potentiaalista bentoniitissa ja kalibrointikäyrästä. Mekaanisesti kaikki tutkitut elektrodit olivat tarpeeksi vahvoja puristetussa bentoniitissa tehtävään mittaukseen tiheyteen 1.66 g/cm³ asti, mutta potentiaalilin stabiilisuus oli ongelma monissa tapauksissa. Poikkeus oli kloridielektrodi, jonka potentiaalikäyrät tasaantuivat bentoniitissa tyypillisesti 1 – 2 päivässä ja pysyivät vakiona mittauksen ajan. Myös kalibrointikäyrät ennen ja jälkeen kokeen olivat lähellä toisiaan. Bentoniitissa ioniselektiivisellä elektrodilla mitatut kloridipitoisuudet olivat selvästi korkeampia kuin pitoisuudet, jotka saatiin olettamalla kloridin homogeeninen jakautuminen huokosveteen. Ioniselektiivisillä elektrodeilla tehdyistä mittauksista lasketut kloridin huokoisuudet vastasivat eksklusiokokeista aikaisemmin saatuja tuloksia. Todennäköinen selitys on, että kloridi jää negatiivisen varauksensa johdosta pienten interlamellaarihuokosten ulkopuolelle ei-interlamellaarihuokosiin, jossa ioniselektiiviset elektrodit mittaavat pitoisuuden. Kalsiumin, sulfaatin ja natriumin potentiaalit stabiloituivat paljon hitaammin kuin kloridielektrodit, kalibrointikäyrät ennen ja jälkeen kokeen olivat monissa tapauksissa kaukana toisistaan ja saadut tulokset olivat epäluotettavia.

Avainsanat: Bentoniitti, huokosvesi, ioniselektiivinen elektrodi.

TABLE OF CONTENTS

ABSTRACT
TIIVISTELMÄ

1	INTRODUCTION	3
2	BENTONITE PROPERTIES	5
2.1	Composition and microstructure of bentonite	5
2.2	Porewater chemistry in bentonite	8
3	ION-SELECTIVE ELECTRODES	11
4	EXPERIMENTAL	15
4.1	General	15
4.2	Preparation and calibration of the electrodes	15
4.2.1	Chloride electrode	15
4.2.2	Sulphate electrode	17
4.2.3	Sodium electrode	18
4.2.4	Calcium electrode	19
4.3	Measurements in bentonite	21
4.3.1	Measurement arrangements	21
4.3.2	Results of chloride and calcium electrodes	23
4.3.3	Results of sulphate and sodium electrodes	29
5	SUMMARY AND DISCUSSION	31
	REFERENCES	35
	APPENDIX A	41
	APPENDIX B	49

1 INTRODUCTION

The spent nuclear fuel from Finnish power plants at Loviisa and Olkiluoto is planned to be disposed of using the KBS-3 concept (Posiva 2010). The waste will be encapsulated in copper-iron canisters placed in deposition holes at about 400 m depth in crystalline bedrock. The space between the canister and the bedrock will be filled with bentonite. Many of the performance targets of the bentonite buffer in the KBS-3 concept are coupled to processes that occur in the water-saturated bentonite. Examples of such processes are the swelling of bentonite, dissolution and precipitation phenomena and transport of water, colloids and ions through the clay. The performance assessment evaluates the processes in a long-term perspective in order to guarantee that the set targets are not seriously impaired by future physico-chemical changes in the repository.

Bentonite porewater chemistry has been studied in the nuclear waste programmes for at least 25 years (Wanner 1987, Snellman et al. 1987, Curti 1993, Wieland et al. 1994, Ohe & Tsukamoto 1997, Muurinen & Lehtikoinen 1999, Bruno et al. 1999, Bradbury & Baeyens 2003, Fernandez et al. 2004). Both experimental methods and modelling have been used in those studies, but general agreement on the composition of the porewater has remained somewhat uncertain. There are many reasons for that uncertainty. The huge swelling pressures in compacted bentonite mean that porewater samples are difficult to extract from it. The different types of porosities mean in micro-scale different types of porewaters, which will be mixed while attempting to squeeze water out from the bentonite for analysis. Direct measurements on water composition in bentonite are exceedingly difficult to perform because of the huge swelling pressure, which the sensors cannot withstand, and the low amount of free water available for the sensor. The majority of experimental data is based on batch experiments with low solid-to-liquid ratio or on the samples squeezed out from compacted clay. Both methods include potential sources of errors. Geochemical modelling has then been offered as a solution, but this approach also includes a lot of uncertainties caused by the exceptional conditions in the clay. However, much has been learned during the past years and the porewater composition can be evaluated, if not yet strictly quantitatively, at least semi-quantitatively by combining the knowledge of the experimental studies, the geochemical modelling, knowledge of the bentonite pore structure and surface properties. Also direct methods for determination of pH and Eh in compacted bentonite have been developed and used for characterization of the conditions in bentonite (Muurinen and Carlsson 2007, 2010). The aim of this study was to develop and test new ion-selective electrodes for measuring the chemical conditions in the porewater of compacted bentonite.

2 BENTONITE PROPERTIES

2.1 Composition and microstructure of bentonite

Table 1 presents the typical mineral composition of the MX-80 bentonite which has been studied as a potential buffer material for many years. The major component of bentonite is montmorillonite, which confers its swelling properties. Other components can play an important role in determining the buffer porewater composition. The buffer around the canisters will be installed as partly water-saturated rings and blocks. The bulk density after full saturation is planned to be 1 950–2 050 kg/m³ (Juvankoski 2010).

Montmorillonite has a 2:1 layer structure consisting of one octahedrally co-ordinated sheet between two tetrahedrally co-ordinated sheets. By definition (Newman 1987, Karnland et al. 2006), the octahedral sheet has aluminium as the central ion, which is partly substituted principally by magnesium. The tetrahedral sheet has silicon as the central ion, which may partly be substituted principally by aluminium. The substitutions result in a net negative charge of the montmorillonite layer in the range of 0.4 to 1.2 unit charges per O₂₀(OH)₄ -unit, and the octahedral charge is larger than the tetrahedral. The induced negative layer charge is balanced by cations (c) located between the individual layers (interlayer space). A variable number (n) of water molecules may be intercalated between the individual mineral layers. The montmorillonite ideal formula may consequently be written:

(Si_{8-x} Al_x) (Al_{4-y} Mg_y Fe) O₂₀(OH)₄ c_{x+y} n(H₂O), where (x < y) and 0.4 < x+y > 1.2.

Table 1. Typical content of some major mineral phases in MX-80 bentonite (Karnland et al. 2006).

Phase	MX-80
Bentonite	
Montmorillonite (%)	81.1 – 82.3
Illite (%)	0.6 – 0.7
Kaolin (%)	
Calcite (%)	0.1 – 0.5
Gypsum (%)	0.5 – 1.3
Pyrite (%)	0.5 – 0.6
Quartz (%)	2.5 – 3.6
Exchangeable cations of	
CEC (meq/g)	0.71 – 0.77
Na (%)	83
K (%)	2
Ca (%)	9
Mg (%)	6

Parallel montmorillonite layers form particles (or stacks) which can be defined as a dense assembly of layers with strong orientational correlations. The particles form assemblies called aggregates, which can be defined as an assembly of particles with mechanical cohesion but little orientational correlation (Salles et al. 2009). Accordingly, one can distinguish between interlamellar porosity, inter-particle porosity and inter-aggregate porosity (Wersin 2003, Bradbury and Baeyens 2003, Tournassat and Appelo 2011).

The generalized microstructure of MX-80 clay of compacted powder grains proposed by Wersin (2003) is seen in Figure 1. The compacted clay in contact with water takes water into the interlamellar spaces thus reducing the volume of the larger pores. Depending on the available space and on the type of adsorbed cation, the interlamellar space varies from about 0.6 to 0.9 nm while the thickness of the montmorillonite layer is about 1 nm. The exchangeable cations are in any case bound to the vicinity of the montmorillonite surfaces because of the demand of the electrical neutrality.

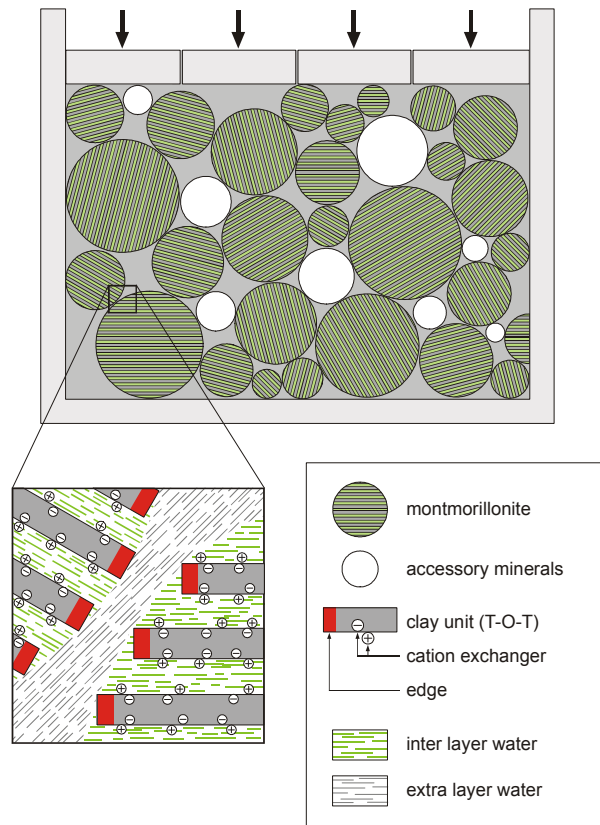


Figure 1. Generalized microstructure of MX-80 (Wersin 2003).

The microstructure of bentonite has been studied using various experimental methods like x-ray diffraction (XRD), small angle x-ray spectroscopy (SAXS), neutron diffraction, nuclear magnetic resonance spectroscopy (NMR), scanning electron microscopy (SEM), transmission electron microscopy (TEM), adsorption isotherms and anion exclusion measurements. As far as partly or fully water-saturated bentonite is

concerned, the microstructure has been difficult to study because the different pore types are sensitive to changes in the water content, and aggregates and particles can break thus forming new pores.

The determination of interlamellar and non-interlamellar water in bentonite and in montmorillonite was considered in the NMR studies by Montavon et al. (2009) and Ohkubo et al. (2008). In the study by Muurinen and Carlsson (2013) NMR, SAXS and chloride exclusion were used to study the pore structure of bentonite. The results by NMR indicated for compacted samples with dry densities above 1.0 g/cm^3 , the presence of two main types of porewater, which were interpreted as inter-layer and non-inter-layer water. The NMR studies and SAXS studies coupled with the Cl porosity measurements provide very similar pictures of how the porewater is divided into two phases in bentonite and the IL water and non-IL water are almost the same with both methods. The second-order regression equations presented in the legend of Figure 2 describe well the porosities as a function of the dry density of bentonite within the described density area.

The accessible porosity for anions in bentonite is smaller than the total porosity owing to anion repulsion (exclusion) by the surface of montmorillonite. The diagrams in Figure 2 also show that the chloride porosity is smaller than the non-IL porosity, which indicates the exclusion in the non-IL water, too. The accessible porosity for anions is a function of the bentonite density and the salt concentration, which affects the thickness of the electrical double-layer.

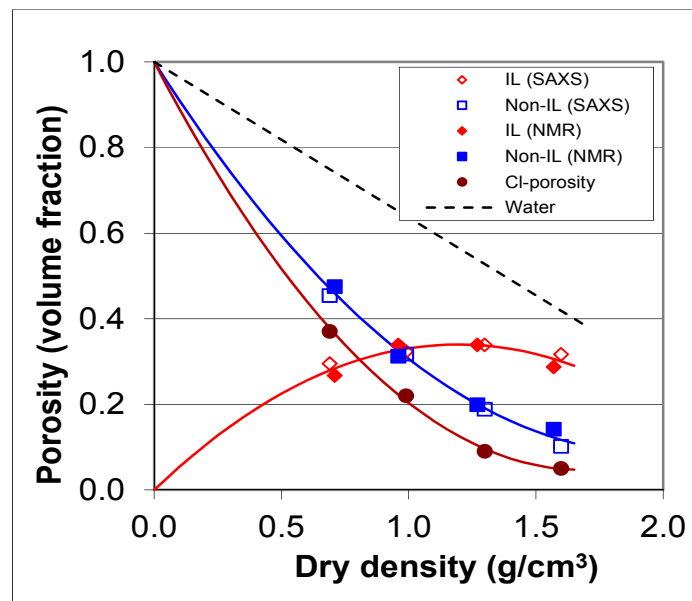


Figure 2. IL, non-IL, water and chloride porosity in MX-80 samples saturated with 0.1 M NaCl solution at different dry density. The IL and non-IL porosities were evaluated from SAXS and NMR measurements. The layer model was used for bentonite in SAXS modelling. The trend lines are IL: $y = -0.2231x^2 + 0.541x$; $R^2=0.981$, non-IL: $y = 0.223x^2 - 0.905x + 1$; $R^2 = 0.997$, Cl porosity: $y = 0.337x^2 - 1.133x + 1$; $R^2=0.999$ (Muurinen and Carlsson 2013).

Anion exclusion is well known in soil science and the Gouy-Chapman theory for the diffuse double layer has been applied to model anion exclusion in clay suspensions, for example in Bolt and Warkentin (1958), Edwards and Quirk (1962), Bolt and De Haan (1982). Sposito (1982) improved the Gouy-Chapman model by adding the distance of minimal approach, owing to the ion size. Birgersson and Karnland (2009) used the Donnan equation to calculate the exclusion in compacted bentonite in contact with an external NaCl solution using uniform porosity in the bentonite. In Muurinen et al. (2007) and Muurinen et al. (2009) the Donnan model was used for the experiments with compacted bentonite assuming two different pore types in bentonite. The anion exclusion has also been observed in many diffusion experiments performed in compacted bentonite (Eriksen and Jacobsson 1984, Muurinen 1994, Kozaki et al. 2001, Moleira et al. 2003, Van Loon et al. 2007). In Tournassat and Appelo (2011), anion exclusion data were gathered from the literature, reprocessed and modelled using different models. It was concluded that those models that consider a heterogeneous pore distribution reproduce the data better over a wide range of conditions than models which assume a homogeneous bentonite. The number of layers in the stacks is a variable that remains to be related to sample preparation and experimental conditions.

2.2 Porewater chemistry in bentonite

During recent years, many studies have been carried out on the chemical interactions between bentonite and groundwaters (Snellman et al. 1987, Takahashi et al. 1987, Melamed et al. 1992, Sasaki et al. 1995, Muurinen et al. 1995, and Muurinen et al. 1996). The conditions cover compacted and non-compacted bentonites, different water compositions, water-bentonite ratios, and bentonite types and temperatures. The present approaches in modelling the chemistry of bentonite porewater are mostly based on simple thermodynamic models that include equilibrium reactions with trace accessory minerals (calcite, quartz, kaolinite), soluble sulphate and chloride salts, ion exchange and protonation-deprotonation reactions of the montmorillonite edge sites (Wanner (1987), Wieland et al. (1994) and Curti (1993), Ohe and Tsukamoto (1997), Wersin 2003, Bradbury and Baeyens 2003, Domènech et al. 2004, Luukkonen 2004). Figure 3 presents schematically the geochemical equilibrium processes used in modelling.

The conditions in the porewater of compacted bentonite differ from those in the interaction experiments using soft clay and a low bentonite-to-water ratio. Most of the water in compacted bentonite is chemically bound for hydration of the exchangeable cations in the narrow interlamellar spaces of the montmorillonite. Only some of the pores are so large that the water can be considered as free. It is usually assumed that the amount of water involved in the geochemical processes in bentonite corresponds to the water in the large external pores, while free ions are strongly excluded from the interlamellar space. The exchangeable cations of the interlamellar space participate in the development of the porewater chemistry by diffusion and cation-exchange processes, however. Usually the geochemical porosity is supposed to be equivalent to the accessible porosity of chloride. The amount of that porosity depends then on the dry density and salinity in the system. At the dry density planned to be used for the buffer in the disposal of nuclear wastes ($> 1.5 \text{ Mg/m}^3$), the external porosity in freshwater conditions is assumed to be a few per cent (Muurinen 1994, Bradbury and Baeyens 2002, Curti and Wersin 2002, Fernández et al. 2004) and can increase up to 10 % in

saline groundwater conditions where the double layers are thinner. The thickness of the electrical double layer on the montmorillonite surface based on Gouy-Chapman model is about 0.3, 1.5 and 6 nm in 1.0, 0.1 and 0.01 M 1:1 electrolytes, respectively (Tournassat and Appelo 2011).

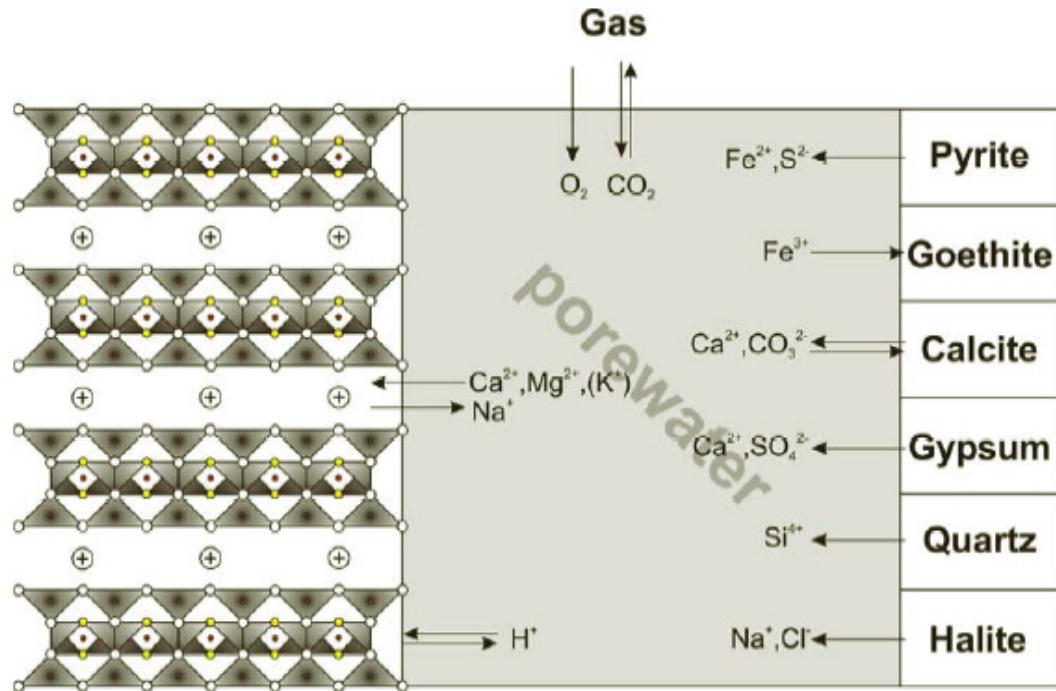


Figure 3. Schematic illustration of geochemical equilibrium processes used in modelling by Luukkonen (2004). The montmorillonite layering and interlayer sites are seen on the left, the mineral equilibria on the right and the entrapped gases on the top.

3 ION-SELECTIVE ELECTRODES

Ion-selective electrodes (ISE) are sensors that convert the chemical activity of an ion in a solution into an electrical potential. The potential is theoretically dependent on the logarithm of the chemical activity of the ion, according to the Nernst equation seen in equation 1. In the equation, E is the measured potential, E_0 is a constant determined by the measurement arrangement, R is the gas constant, T is absolute temperature, z is the charge of the ion, F is the Faraday constant and a is the activity of the ion in the solution. A complete measurement arrangement comprises an ion-selective electrode, reference electrode and a voltmeter for measurement of the potential difference between the two electrodes. At the temperature of 25 °C the slope has a value of 59.16 mV when the charge of the ion is one.

$$E = E_0 + \frac{2.303RT}{zF} \log a \quad (1)$$

Selectivity is the ability of the sensor to respond to one species (analyte) in the presence of an interfering species. If the concentration of the interfering species increases, the detection limit of an analyte shifts to a higher concentration. The selective layer of the sensor should be such that the detection limit is low and the measuring range wide. It is important to note that the potential depends on the activity and not on the concentration of the analyte.

Different types of ion-selective membranes have been studied and developed for the electrodes, and they are often classified according to the physical state as solid or liquid membranes (Janata 2009). Pungor (1997) has classified ion-selective electrodes in a somewhat different way as

- a) precipitate or crystal-based electrodes (e.g. silver halides, silver sulphide, LaF_3 etc),
- b) acid-base electrodes (e.g. glass electrodes, etc)
- c) electrodes based on complex formation (e.g. valinomycin, polyethers, etc).

Groups a) and b) belong to the solid-state membranes, while c) belongs to the liquid state membranes.

Historically, interest was first directed to solid membranes. The first description of such a phenomenon was the observation that various acidic and alkaline solutions produce a potential on the surface of glass (Haber and Klemensiewicz 1909). The oldest and most important member of this group is the glass pH electrode, where the proton-binding sites are created by the defects in the SiO_2 matrix caused by non-silicon constituents (Janata 2009). When the glass membrane is exposed to water, a hydrated layer is formed on the surface. There are two processes, ion exchange and diffusion, which contribute to the value of the membrane potential (Janata 2009).

Kolthoff and Sanders (1937) proposed fused silver chloride and silver bromide discs for the detection of chloride and bromide. The first real ion-selective electrodes were prepared at the beginning of the 1960s and Pungor and Tóth (1973) have reviewed studies on such electrodes. The precipitate-based electrodes can be prepared in three ways: from single crystals, from pressed crystals, and from crystals embedded in a suitable binding material. The first two kinds of electrodes form a group of

homogeneous electrodes, while the third type gives the heterogeneous electrodes. Examples of the solids used in homogeneous electrodes are AgCl, AgBr, LaF₃, Ag₂S and CaF₂+LaF₂ for measurement of Cl⁻, Br⁻, F⁻, S²⁻ and Ca²⁺, respectively. Essential to the sensor materials is the low solubility in the measurement conditions. In the case where there are also other anion(s) that form an insoluble compound with the membrane cation the membrane is gradually partially covered by the disturbing precipitation and a mixed potential is formed. Silicon rubber and different polymers were often used as the embedding materials in preparation of the heterogeneous electrodes. However, the precipitate-type electrodes can be prepared only for a small number of ions owing to the lack of suitable low-solubility precipitates.

Nowadays, more interest has been directed to polymer-based membranes which contain different carriers. These membranes can be tailored for different ions and consequently they are available for more ions than precipitate-type electrodes. The binding sites are more or less mobile complexing agents, called ionophores, which are dissolved in a suitable solvent and trapped in an organic matrix. They can be charged or neutral ones. The primary interaction between the ion in water and the hydrophobic membrane containing the ionophore is the extraction process driven by the chemical affinity of the ion for the membrane. The most common polymer matrix is poly(vinyl chloride) which comprises typically 30 wt% of the membrane. The remaining major component is the solvent (plasticizer). The ionophore usually comprises 1% of the membrane. Other membrane components include large hydrophobic anions (Janata 2009). Such electrodes are reviewed in Bakker et.al (1997), Bühlmann et al. (1998), Bakker (2004) and Bobacka et al. (2008).

Figure 4 presents different construction principles for ion-selective electrodes (Bobacka 2006). The classical ISE with internal filling solution (Fig. 4 a) works well in normal laboratory conditions but needs refilling and cannot be miniaturized. In the case of the hydrogel electrode the filling solution is replaced with a hydrogel (Fig. 4 c). The other electrode types, like the coated-wire (Fig. 4 b) and its modifications (Fig. 4 d,e,f) where an intermediate layer is used between the electronic conductor and the ion-selective membrane in order to improve the electrode properties, offer better alternatives for miniaturizing.

Compacted bentonite sets special requirements for the ISEs used in the measurements. The high swelling pressure, which can rise to several MPa can break the electrode or change the properties of the ion-selective membrane. The content of the solid material can rise at the planned buffer density to 55 – 60 volume% such that the membrane is in contact with both the solid material and the porewater. Most of the porewater is, however, interlamellar, which cannot be in direct contact with the electrode. The measurement times have to be rather long, in many cases weeks or months, and the electrodes cannot be calibrated during the measurement, which sets requirements on the potential stability. Possible solutions for the instability have been dealt for example in Oesch et al. (1986), Bobacka (2006), Crespo et al. (2008), Jaworska et al. (2011), Ivanova et al. (2012) and Zhou et al. (2012).

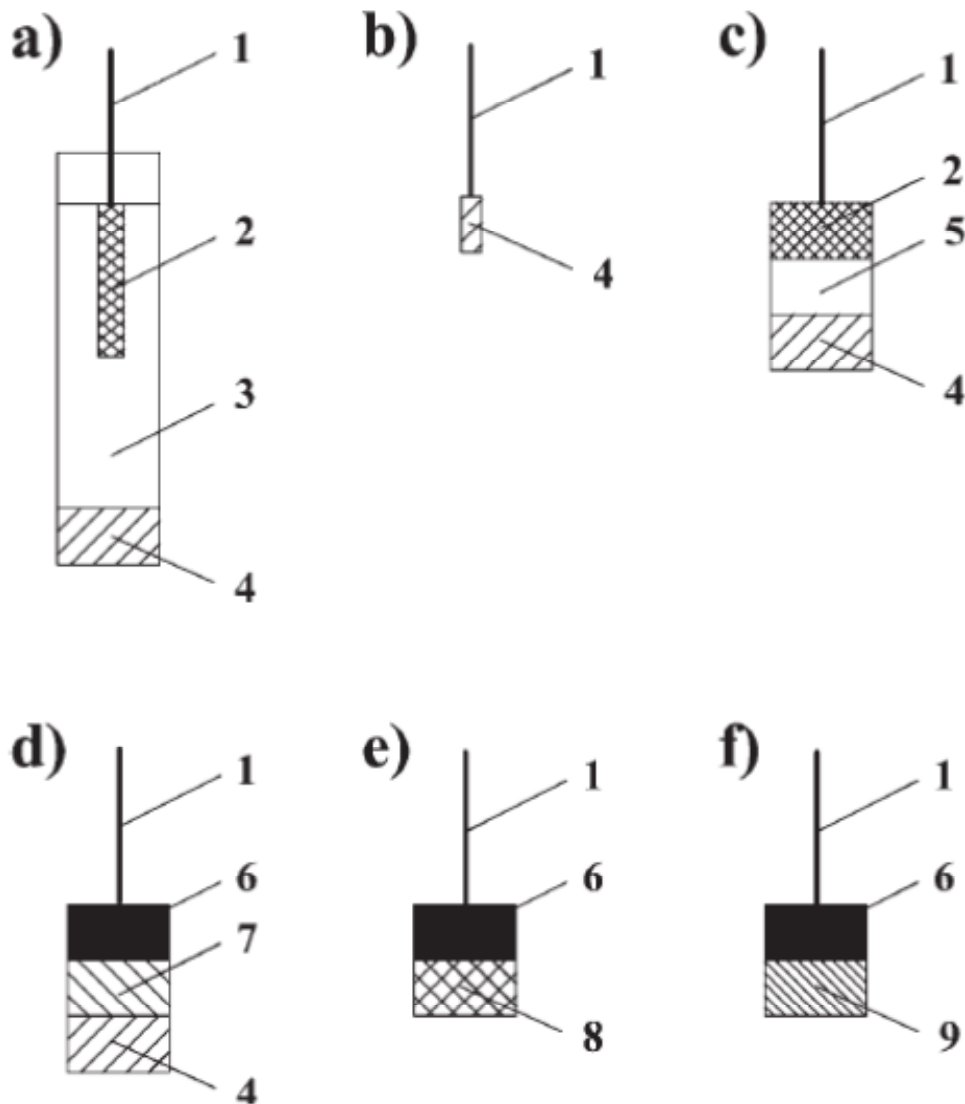


Figure 4. Construction principles for ion-selective electrodes (ISEs) (Bobacka 2006): a) conventional ISE with an internal reference electrode and internal filling solution, b) coated wire ISE, c) ISE with a hydrogel contact, d) ISE with a conducting polymer contact, e) ISE with a conducting polymer dissolved in the ion-selective membrane, f) ISE with a (functionalized) conducting polymer as sensing membrane. Construction parts of the electrodes: 1) electronic conductor, 2) internal reference electrode, 3) inner filling solution, 4) ion-selective membrane, 5) hydrogel, 6) electronic conductor with a high work function, 7) conducting polymer, 8) ion-selective membrane containing a conducting polymer, 9) conducting polymer containing ion-recognition sites (ionophores).

Very few measurements have been performed in compacted swelling clays under high pressure. An IrOx electrode has been developed for pH measurement in compacted, water-saturated bentonite by Muurinen and Carlsson (2007). In the bentonite samples where the pH was adjusted with 1 M NaOH solution (Muurinen and Carlsson 2010), approximately similar values were obtained in the bentonite and the squeezed

porewater. In tests on bentonite samples prepared from bentonite and deionized water, where the pH was measured under varying bentonite-to-water ratios in batch experiments or compacted clay, the modelling curve calculated with the geochemical code PHREEQC equates well with the measured pH values.

The feasibility of using a potassium ion-selective electrode to monitor changes in a solution of potassium concentration in soil suspensions with time, under shaking conditions, was investigated by Wang and Huang (1990). The effect of suspended soil particles on the K-ISE method was negligible for soil suspensions with a solution/soil ratio of 50:1 (ml/g).

Angst and Vennesland (2009) studied the disturbance caused by diffusion potentials (liquid junction potential and membrane potential) on the result of chloride measurement in concrete with an Ag/AgCl electrode. It was concluded that diffusion potentials can significantly disturb the potential readings. In order to minimize liquid junction potential errors, the chemical composition of the contacting solution should be as similar to the pore solution as possible. Concentration gradients between the measuring sensor and the reference electrode lead to membrane potentials. The potential error can be minimized by placing the electrodes close to each other.

The most interesting ions for which electrodes should be found in the bentonite are Na^+ , Ca^{2+} , Mg^{2+} , Cl^- , SO_4^{2-} and HCO_3^- . The electrodes should be strong enough to withstand the pressure caused by the bentonite and be stable enough to allow measurements of at least a few weeks. Table 2 summarizes the most promising precipitate or crystal-based electrodes on the basis of the literature which might be suitable for measurements in bentonite. The selected electrodes are homogeneous without any matrix material because they are probably more reliable in the conditions of the high swelling pressure. No suitable precipitate-type electrode was found for HCO_3^- .

Table 2. *The most promising precipitate and crystal-based electrodes for measurements in bentonite.*

Ion	Active material	Matrix	Reference
Na^+	$\text{Na}_x\text{Mo}_6\text{O}_{17}$	Crystal	Shuk et al. (1996)
Na^+	Nasicon	Sintered powder	Caneiro et al. (1991)
Ca^{2+}	$\text{Na}_{1+x}\text{Zr}_2\text{Si}_x\text{P}_{3-x}\text{O}_{12}$ $\text{CaF}_2 + \text{LaF}_3$	CaF_2 coating on LaF_3	Farren 1972(patent) (Na, Mg disturb)
Mg^{2+}	$\text{MgF}_2 + \text{LaF}_3$	MgF_2 coating on LaF_3	Farren 1972(patent) (Na, Ca disturb)
Cl^-	AgCl	Compacted mixture of Ag and AgCl powder	In Vivo Metric, Healdsburg, California, USA
SO_4^{2-}	Ag_2S , PbS , PbSO_4 , Cu_2S	Compacted powder	Mohan and Rechnitz (1973)

4 EXPERIMENTAL

4.1 General

The earlier experiences with the IrOx electrode for pH measurement and some pre-tests with Ag/AgCl electrodes for chloride measurement in compacted bentonite suggested that the inorganic precipitate-type electrodes could withstand conditions in the compacted bentonite. The pre-tests with the polymer-type membrane, on the contrary, indicated that they would not survive in the compacted bentonite without essential improvement of the mechanical strength and stability. The leak-free electrode LF-2 of Innovative Instruments, Inc. Tampa, USA, was used as the reference electrode in the measurements above. The electrode is based on the Ag/AgCl wire in 3.4 M KCl solution and uses a leak-free conductive junction. The electrode body is constructed from PEEK. The focus of the study was then directed to the precipitate-type membrane electrodes. The electrodes were prepared for the measurement of chloride, sulphate, sodium and calcium. The electrode body (see Figure 5) was constructed from a PEEK screw (M8) aimed to be fixed into the measurement cell of the bentonite. A hole was bored through the screw where a PEEK tube for the electric wire was fixed with epoxy. At the end of the screw, a space of 6 mm in diameter and 2.5 mm in height was made for the ion-selective membrane.

The sodium and sulphate electrodes were planned to be used together in Na-bentonite with Na₂SO₄ solution as the porewater, and the electrodes were calibrated in Na₂SO₄ solutions. The calcium and chloride electrodes were planned to be used together in Ca-bentonite with CaCl₂ solution as the porewater, and the electrodes were calibrated in CaCl₂ solutions. The calibrations were done before and after the measurements in the bentonite. Commercial leak-free electrodes LF-2 were used as reference electrodes in all experiments below. The potentials of the LF-2 electrodes were compared systematically with an Orion 900100 reference electrode in order to guarantee the stability. The potentials were presented versus the standard hydrogen electrode (SHE) such that the measurements of different times were comparable with each other.

4.2 Preparation and calibration of the electrodes

4.2.1 Chloride electrode

The chloride electrodes were based on the commercial Ag-AgCl pellets prepared from a fine-grain homogeneous mixture of silver and silver chloride (In Vivo Metric, Healdsburg, California, USA). The pellets were 4 mm in diameter and 2 mm in height with 10 mm silver wire. The silver wire was first soldered to a 7 cm long electric wire and placed into a PEEK tube in a PEEK screw, as seen in Figure 5. The PEEK tube was then filled with epoxy so that also the bottom of the Ag-AgCl pellet was fixed into the PEEK screw. When the epoxy was hardened, the slot between the sides of the Ag-AgCl pellet and the screw was filled with epoxy. A longer electric wire was soldered to the electrode and the join was supported with epoxy.

Figure 6 presents the results of subsequent calibrations of a chloride electrode in CaCl₂ solutions of different concentrations. In the bentonite measurements the electrode was between the calibrations 1 – 2 and 3 – 4. There is some scattering, but as a rule the chloride electrode is very stable in the solution measurements and changes very little also in the bentonite measurement.

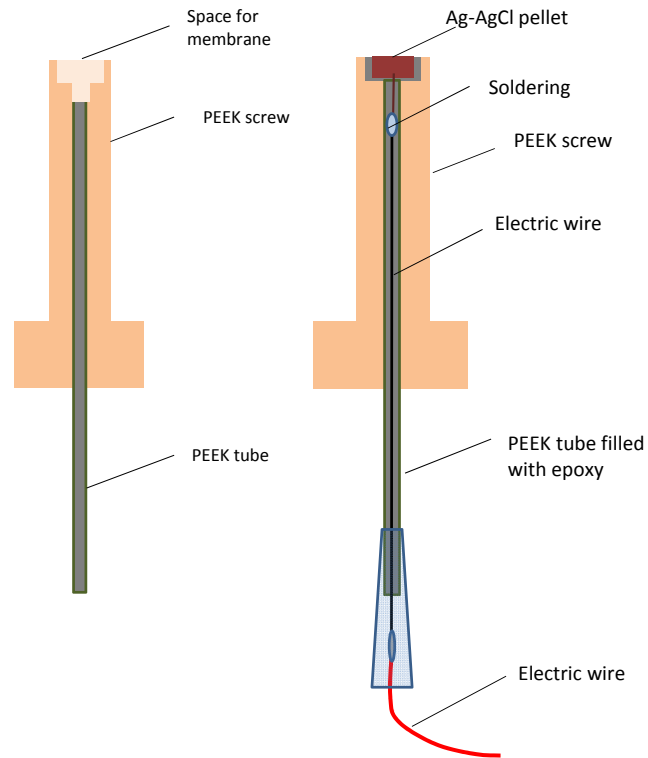


Figure 5. Structure of the chloride electrode. On the left is the electrode body and on the right the complete electrode.

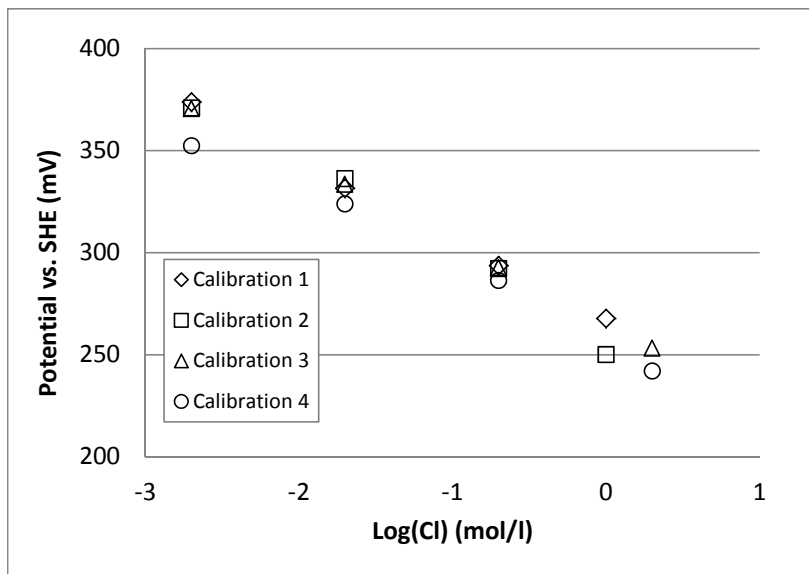


Figure 6. Potentials of a chloride electrode as a function of the logarithm of the chloride concentration of the CaCl_2 solution in four subsequent calibrations. In the bentonite measurements the electrode was between the calibrations 1 – 2 and 3 – 4.

4.2.2 Sulphate electrode

The membranes for the sulphate electrodes were prepared according to Mohan and Rechnitz (1973). The membrane was based on a four-component mixture of PbSO_4 (31.7 mol%), PbS (31.7 mol%), Ag_2S (31.7 mol%) and Cu_2S (4.9 mol%). In order to obtain a homogeneous mixture, the chemicals for several electrodes were first ground together in an Agate mill. The powder was then moved to an anaerobic glove-box in order to avoid oxidation and sorption of humidity. The amount needed by an electrode (270 mg) was placed in an AtlasTM evacuable pellet die of 5 mm in diameter (Specac, River House, UK). The die was first evacuated and heated for two hours at 150 °C without pressing in order to remove gases and traces of water. The pellet was then pressed overnight at 7 000 bar at 150 °C whilst under vacuum. The next day, the pellet was removed from the die and both ends were wet-polished with number 600 abrasive paper. Then the pellet was dried at 100 °C and fixed to the electrode body, as seen in Figure 7. The electrical contact between the membrane and the silver wire in the electrode was made with silver epoxy (World Precision Instruments, USA). When the silver epoxy was hardened, the slot between the sides of the membrane pellet and the PEEK screw was filled with normal epoxy. An electric wire was soldered to the silver wire in the electrode and the joint was supported with epoxy.

The electrodes were immersed overnight in 0.1 M Na_2SO_4 before starting the calibrations in 0.001 – 0.5 M Na_2SO_4 solutions. Figure 8 presents the potentials of a sulphate electrode as a function of sulphate concentration in five subsequent calibrations. The membrane was polished after calibration number 2 with number 600 abrasive paper. In the bentonite measurement the electrode was between the calibrations 4 – 5. There is a clear change in the potentials between the calibrations.

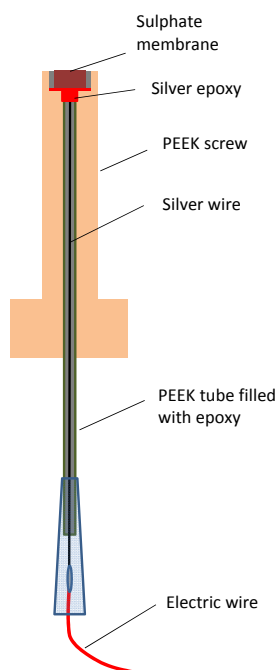


Figure 7. Structure of the sulphate electrode.

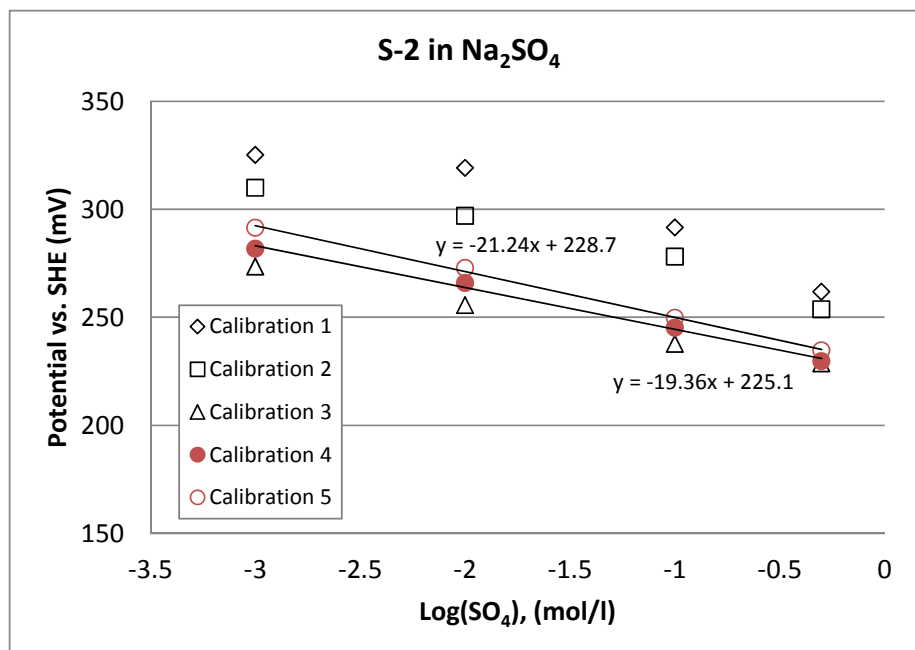


Figure 8. The potential of a sulphate electrode as a function of the logarithm of the sulphate concentration in Na_2SO_4 solutions in repeated calibrations. The numbers of the measurements are given in the legend. The membrane was polished after the second measurement. In the bentonite measurement the electrode was between the calibrations 4 – 5.

4.2.3 Sodium electrode

In the case of sodium, two alternative membrane materials are given in Table 2. Of these, the Nasicon (Natrium Super Ionic Conductor) electrode is easier to prepare and was studied as the first alternative. Preparation of the membrane was based on the paper by Caneiro et al. (1991). Synthesis of the Nasicon ($\text{Na}_{1+x}\text{Zr}_2\text{Si}_x\text{P}_{3-x}\text{O}_{12}$) was done by the method proposed by Colomban (1989) likewise in Caneiro et al. (1991). The starting chemicals, tetraethyl orthosilicate ($\text{Si}(\text{OC}_2\text{H}_5)_4$), zirconium(IV) propoxide ($\text{Zr}(\text{OC}_3\text{H}_7)_4$, 70 % in propanol), and ammonium dihydrogen phosphate ($\text{NH}_4\text{H}_2\text{PO}_4$) were provided by Sigma Aldrich. Stoichiometric amounts of the chemicals above and NaOH as 1 M solution were used in the synthesis. First, $\text{Si}(\text{OC}_2\text{H}_5)_4$ was mixed with $\text{Zr}(\text{OC}_3\text{H}_7)_4$ and $\text{NH}_4\text{H}_2\text{PO}_4$ with the 1-molar NaOH. Both mixtures were then heated in a water bath to 70°C and quickly mixed together. The precipitation reaction is quick and produces white Nasicon powder. The Nasicon was washed four times with water, and the powder was separated with a centrifuge between the washings. Finally, the separated powder was washed four times with acetone in order to remove the water. The acetone left in the Nasicon after the last centrifuging was first allowed to evaporate at room temperature and finally dried at 70°C . The product was stored in a desiccator until used for preparation of the electrodes.

Before using the Nasicon for the preparation of the membranes, the powder was once again dried at 105°C . About 100 mg of the dried Nasicon was placed into the pressing die and kept for an hour at 200°C under vacuum without pressing. Then the powder

was pressed for two hours at 4 000 bar. The pellet was moved on a platinum plate and sintered in an oven where the temperature was increased within four hours from room temperature up to 1 000 °C, and then kept at 1 000 °C for an hour before being allowed to cool for twelve hours. Both ends of the pellets were wet-polished with number 280 abrasive paper. The pellet was washed in an ultrasonic bath and dried at 100 °C. The pellet was fixed with silver epoxy and epoxy to the electrode body in the same way as the sulphate membrane presented in Figure 7.

Figure 9 presents the calibration results of a sodium electrode as an example of the behaviour of the electrodes during repeated measurements. Both the slope and the constant of the curve change during the calibrations. After the second measurement the membrane was polished with number 280 abrasive paper, which clearly changed the potentials. In the bentonite measurement the electrode was between the calibrations 4 – 5. The change in the bentonite was clearly larger than in the solutions.

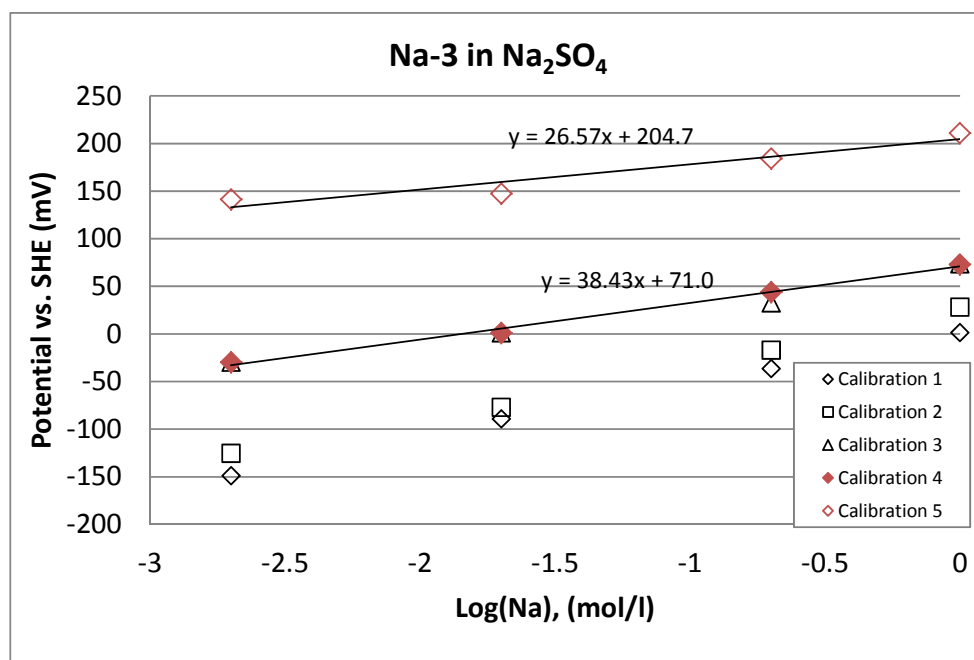


Figure 9. The potential of a sodium electrode as a function of the logarithm of the sodium concentration in the Na_2SO_4 solution in repeated calibrations. The numbers of the measurements are given in the legend. The membrane was polished after the second calibration and in the bentonite measurement the electrode was between the calibrations 4 – 5.

4.2.4 Calcium electrode

The problem in using CaF_2 as an ion-selective membrane in a calcium electrode is that it is not a semiconductor. According to Farren (1972), it is possible to couple CaF_2 , however, with a semiconductor (like LaF_3) for preparation of a calcium electrode. In this study we used commercially available europium-doped LaF_3 pellets (Crystran Ltd, UK) as a starting material and coated them with colloidal CaF_2 in order to change them for calcium electrodes. The pellets were 5 mm in diameter and 2 mm in height.

The calcium fluoride nanoparticles used in the coating were prepared according to the method in Tahvildari et al. (2012). Calcium chloride (0.01 mol $\text{CaCl}_2 \cdot 2\text{H}_2\text{O}$) and ammonium fluoride (0.02 mol NH_4F) were mixed separately in 50 ml of ethanol. The NH_4F solution was added into the CaCl_2 solution in a conical flask whilst stirring. The mixing was continued for several hours to gradually transform the solution into a white suspension. The non-dissolved CaCl_2 and NH_4F were first removed by a quick sedimentation. Then the colloidal CaF_2 was separated in a centrifuge, washed four times with water in order to remove the chloride and ammonium ions, and three times with ethanol in order to remove the water. The colloidal CaF_2 was finally left in the ethanol.

Approximately 1 mg of CaF_2 in $7 \times 3 \mu\text{l}$ volumes of ethanol was pipetted on to one end of the $\text{La}(\text{Eu})\text{F}_3$ pellet. Ethanol was allowed to evaporate away between each pipetting. The pellet was then heated on a platinum plate to 400°C in an hour, kept at that temperature for an hour and then cooled to room temperature in 16 hours. The pellet was fixed with silver epoxy in the electrode body in the same way as the sulphate membrane seen in Figure 7. The electrode was kept in 0.1 M NH_4F solution overnight before starting the calibrations in the solutions.

Figure 10 presents the potentials of a calcium electrode in subsequent calibrations in CaCl_2 solutions. In the bentonite measurements the electrode was between the calibrations 3 – 4 and 5 – 6. It is obvious that the calcium electrode is not very stable, which at least partly may be caused by the loss of the CaF coating from the membrane.

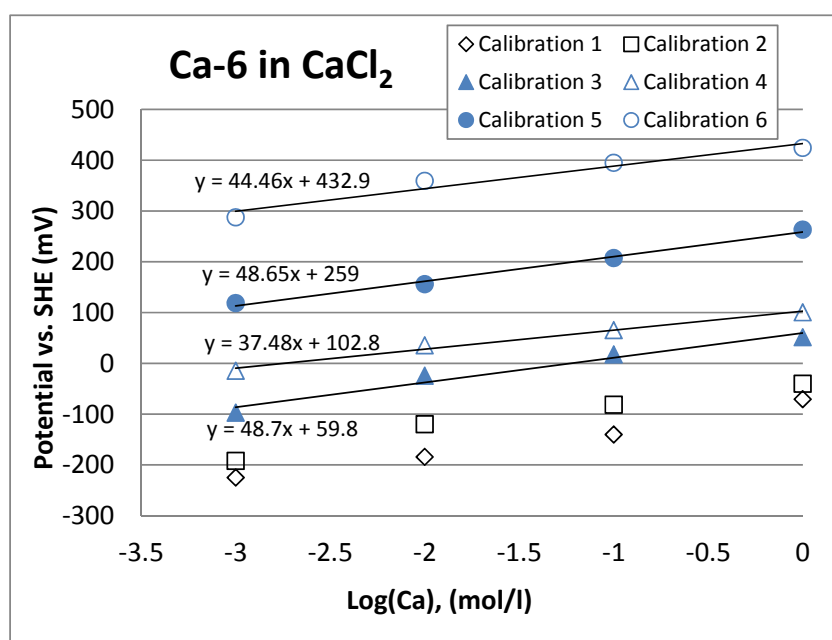


Figure 10. The potential of a calcium electrode as a function of the logarithm of the calcium concentration in CaCl_2 solution in repeated calibrations. The numbers of the measurements are given in the legend. In the bentonite measurements the electrode was between the calibrations 3 – 4 and 5 – 6.

4.3 Measurements in bentonite

4.3.1 Measurement arrangements

The dissolving components of natural bentonite can create complex chemical conditions in the porewater. In order to avoid the problem, the bentonites aimed for the electrode tests were purified by trying to remove the easily dissolving components like gypsum and chlorides and by changing the montmorillonite to sodium or calcium form. The purified sodium bentonite was prepared from MX-80 sodium bentonite by washing it with 0.5 M NaCl solution. Washing was carried out in one-litre centrifuge bottles. In each bottle 50 g of MX-80 and 600 ml NaCl solution was weighed. The bottles were shaken overnight, the bentonite was separated in the centrifuge and the supernatant removed. The washing was repeated four times. Then washing was continued with deionized water as long as separation of the bentonite was possible. Removal of the dissolved ions was continued with dialysis until the conductivity was <0.04 mS/cm. The calcium bentonite was prepared from the purified sodium bentonite by changing it to the calcium form with 0.5 M CaCl_2 solution. The excess CaCl_2 was removed by washing several times with deionized water and finally by dialysis.

The compacted samples for the measurements with the ion-selective electrodes were prepared from the purified clays in a squeezing cell, as seen in Figure 11. During the compaction, the hole for the measurement electrode was closed with a screw and the reference electrode was replaced with a syringe.

Suitable amounts of the bentonite powder and solution were mixed to obtain a sample of the desired dry density and ion concentration. The weights of the bentonite and volumes of the solution needed in the preparation were evaluated from Equations 2 – 5.

$$\rho_d = \frac{m_b}{V_{tot}} \quad (2)$$

$$V_{tot} = V_s + V_b \quad (3)$$

$$V_b = m_b / \rho_b \quad (4)$$

$$V_s = m_s / \rho_s \quad (5)$$

When the volume of the sample (V_{tot}) and dry density (ρ_d) are decided the weight of the needed dry bentonite (m_b) is obtained from Equation 2. The volume taken by the bentonite is calculated from Equation (4), where ρ_b is the grain density of bentonite (2.75 g/cm^3). The volume of the solution (V_s) can then be calculated from Equation (3). A value of 1 g/cm^3 was used for the solution density (ρ_s). In the case of the sodium bentonite, Na_2SO_4 solutions of different concentrations were added to the bentonite, and sodium and sulphate concentrations were the measured ions. In the case of calcium bentonite, CaCl_2 solutions were added to the bentonite, and calcium and chloride concentrations were the measured ions. The bentonite-solution mixture was compacted, and pressing was continued a few days such that some porewater was squeezed out from the sample through the reference electrode hole in order to guarantee a complete saturation. Then the screw was removed from the hole of the measurement electrode and the measurement electrode was turned into the hole. The piston was pressed briefly in order to obtain good contact between the bentonite and the electrode. The piston was

finally fixed at a certain position with the support, and the LF-2 reference electrode was put in place. Table 3 presents the properties of the samples prepared for the measurements with different electrodes. The dry density values are based on the water content measurement of the bentonite after the measurement (see below). Each calcium and chloride electrode was used twice in the bentonite measurements, while the sodium and sulphate electrodes were used only once.

The potential differences between the measurement and reference electrode were measured with a multichannel voltmeter. Approximately once per week the potentials of the reference electrodes were monitored. Simultaneously, the gas bubbles which tended to accumulate in the solution tube between the reference electrode and the bentonite sample were removed. The potential measurements were continued for a few weeks. Then the experiments were finished and the sample cells were opened. A sample was cut from bentonite for water content measurement done by drying the sample at 150 °C. The dry densities of the samples were calculated from Equations 2 – 5 on the basis of the water content measurement. The difference between the weights of a bentonite sample before and after drying give the weight of the water content in the sample and Equation 5 gives the volume of the solution (V_s). The weight after drying is m_b and V_b is obtained from Equation 4. The V_{tot} is given by Equation 3 and the dry density can then be calculated from Equation 2. Another sample was cut from the bentonite for determination of the dissolved components in the bentonite by dispersing the bentonite in deionized water.

The electrodes were released from the bentonite by cutting first the major part of the bentonite away and finally by washing the bentonite away with water. The removed electrodes were placed in deionized water for one day in order to remove the bentonite from the membrane surfaces. Then the electrodes were recalibrated. The concentration in the porewater was calculated from the measured potential and the calibration curves.

Table 3. *Samples for the measurements in compacted bentonite with different electrodes.*

Sample code	Bentonite type	Dry density (g/cm ³)	Solution mixed in bentonite	Codes of cation electrodes	Codes of anion electrodes
C2	Ca-bentonite	1.61	0.1 M CaCl ₂	Ca-4	Cl-2
C3	Ca-bentonite	1.14	0.001 M CaCl ₂	Ca-5	Cl-3
C4	Ca-bentonite	1.63	0.001 M CaCl ₂	Ca-6	Cl-5
C5	Ca-bentonite	1.20	0.1 M CaCl ₂	Ca-7	Cl-1
C6	Ca-bentonite	1.51	0.1 M CaCl ₂	Ca-4	Cl-1
C7	Ca-bentonite	1.63	0.1 M CaCl ₂	Ca-5	Cl-2
C8	Ca-bentonite	1.35	0.001 M CaCl ₂	Ca-6	Cl-3
C9	Ca-bentonite	1.62	0.001 M CaCl ₂	Ca-7	Cl-5
N1	Na-bentonite	1.20	0.1 M Na ₂ SO ₄	Na-1	S-1
N2	Na-bentonite	1.66	0.1 M Na ₂ SO ₄	Na-2	S-2
N3	Na-bentonite	1.21	0.001 M Na ₂ SO ₄	Na-3	S-3
N4	Na-bentonite	1.64	0.001 M Na ₂ SO ₄	Na-4	S-4

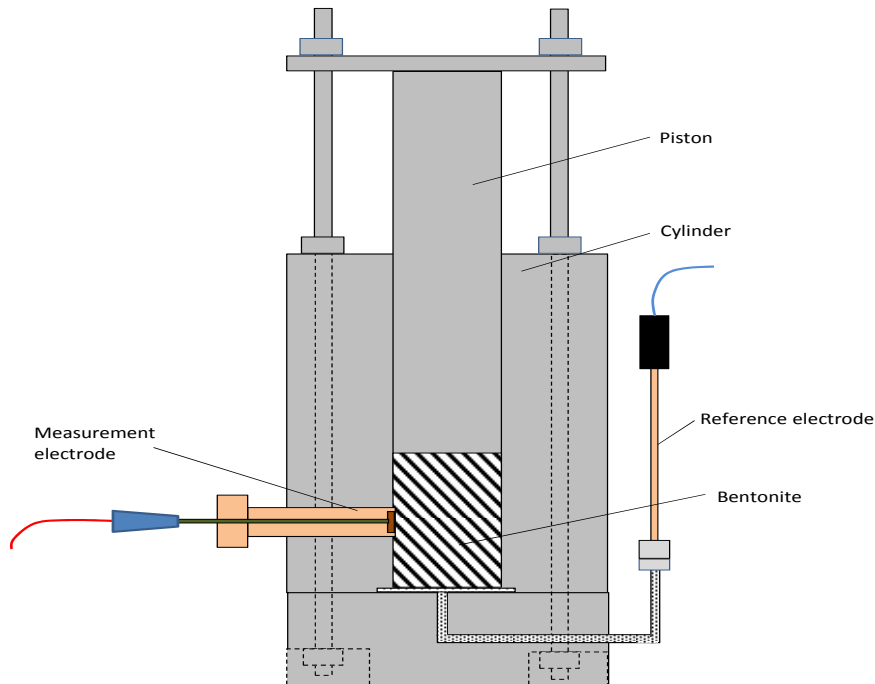


Figure 11. Schematic presentation of the measurement cell for ion-selective electrodes in compacted bentonite.

4.3.2 Results of chloride and calcium electrodes

The results obtained with chloride and calcium electrodes in different bentonite samples are presented in Figures A1 – A8 in Appendix A. Each figure gives the results of one bentonite sample. The figure caption gives first the dry density of the sample and the chloride concentration in dry bentonite (mg/g) determined with the dispersion method.

The uppermost figure (a) presents for each sample the measured potentials of the calcium and chloride electrode as a function of time. The figures (b) and (c) present the calibration curves of the calcium and sulphate electrodes before and after the experiment and the measured potential in bentonite at the end of the measurement. The crossing points of the measured potential line with the calibration curves give the logarithms of the measured concentrations in bentonite on the x-axis. A curve of the “correct calibration” has also been added into the figures for calcium, i.e. a curve which would give to the calcium half of the chloride concentration. This curve is based on the assumption that the chloride electrodes give correct concentrations in the porewater, and the calcium concentration is half of the chloride concentration. The potential curves of chloride in Appendix A stabilize typically in one to two days and stay constant through the measurement. Only in Figure A-9 does the potential change continuously. The calibration curves before and after the experiments are close to each other, too.

The potentials of the calcium electrodes stabilize much more slowly and in many cases continue changing through the measurement. The calibration curves before and after the experiments are in many cases far from each other. In six samples the “correct calibration” is between the pre-calibration and re-calibration curves but in two cases it is outside.

Table 4 presents the chloride and calcium concentrations in bentonite determined with the dispersion method. In the measurement a bentonite sample of about 2 g is dispersed into 20 ml of deionized water such that the dissolved ions in the porewater are diluted to the added water from where they can be analyzed after separation of the bentonite. In the calculations the porewater density was assumed to be 1 g/ml. In the case that an ion is initially fully dissolved in the porewater, its amount can be determined. In the case of chloride one can assume that the ion is initially fully dissolved. In the case of the solubility limited components, ions are produced also by the dissolving ions, which leads to an erroneous result if one wants to evaluate the concentration in the porewater. In the case of calcium, the solubility limited component like calcite can contribute to the concentration in the dispersion water. This appears especially in the cases where the concentration of the added CaCl_2 is low, as seen in Table 4.

Table 4. Chloride and calcium concentrations in sodium bentonite samples C2 – C9 based on the dispersion measurements.

		C2	C3	C4	C5
Weight of wet bentonite sample	g	2.457	1.996	1.867	2.051
Volume of porewater in the sample	ml	0.501	0.677	0.375	0.659
Cl concentration in dispersion water	mmol/l	1.97	0.042	0.026	3.39
Total Cl in dispersion water	mmol	0.051	0.0011	0.0007	0.087
Cl concentration per porewater	mol/l	0.10	0.0016	0.0017	0.13
Cl concentration per dry bentonite	mmol/g	0.026	0.0008	0.0004	0.063
Ca concentration in dispersion water	mmol/l	1.22	0.32	0.32	2.00
Total Ca in dispersion water	mmol	0.031	0.0084	0.0083	0.051
Ca concentration per porewater	mol/l	0.062	0.012	0.022	0.078
Ca concentration per dry bentonite	mmol/g	0.016	0.0064	0.0056	0.037
		C6	C7	C8	C9
Weigh of wet bentonite sample	g	2.054	2.038	2.015	2.059
Volume of porewater in the sample	ml	0.472	0.406	0.552	0.415
Cl concentration in dispersion water	mmol/l	2.06	1.83	0.031	0.034
Total Cl in dispersion water	mmol	0.043	0.038	0.0006	0.0007
Cl concentration per porewater	mol/l	0.090	0.093	0.0012	0.0017
Cl concentration per dry bentonite	mmol/g	0.027	0.023	0.0004	0.0004
Ca concentration in dispersion water	mmol/l	1.37	1.35	0.40	0.42
Total Ca in dispersion water	mmol	0.028	0.028	0.0083	0.0087
Ca concentration per porewater	mol/l	0.060	0.068	0.015	0.021
Ca concentration per dry bentonite	mmol/g	0.018	0.017	0.0057	0.0053

The results of the calcium and chloride measurements are collected in Table 5. The sample code and dry density are presented in the first two columns. In the next two columns the calcium and chloride concentration in bentonite determined with the dispersion method are presented. The concentrations are presented as moles per the total porewater volume (mol/l). The concentrations measured with the ion-selective

electrodes are presented in the next three columns. In the case of chloride, the ISE concentrations are based both on the calibration before (Cl_{precal}) and after (Cl_{recai}) the experiment. In the case of calcium, the calibration after the experiment did not give any reasonable values, and the ISE concentrations in the table are based on the calibration before the experiment.

Table 5. Chloride and calcium concentrations in the bentonite porewater determined with the dispersion method and ion-selective electrodes (ISE).

Sample code	Dry density (g/cm ³)	Cl conc. of porewater (dispersion) (mol/l)	Ca conc. of porewater (dispersion) (mol/l)	Cl_{precal} conc. of porewater (ISE, pre-calibr.) (mol/l)	Cl_{recai} conc. of porewater (ISE, re-calibr.) (mol/l)	Ca_{precal} conc. of porewater (ISE, pre-calibr.) (mol/l)
C2	1.61	0.10	0.063	2.60	1.32	2.21
C3	1.14	0.0016	0.012	0.015	0.015	0.521
C4	1.63	0.0017	0.022	0.023	0.029	0.005
C5	1.20	0.13	0.078	0.35	0.46	0.00024
C6	1.51	0.090	0.06	0.74	0.38	0.755
C7	1.63	0.093	0.068	1.24	0.82	(20.2)*
C8	1.35	0.0012	0.015	0.0074	0.0052	2.67
C9	1.62	0.0017	0.021	0.018	0.014	0.019

*Outlier, not presented in the figures.

Figure 12 presents the chloride concentration determined with ISE using the calibration after the experiment (Cl_{recai}) as a function of the values determined using the calibration before the experiment (Cl_{precal}). There is some scattering but the trend suggests that the Cl_{recai} values are about half of the Cl_{precal} values. It is difficult to say which values are the correct ones. In principle there are different places where the electrode can change its properties. The drift can continue and depend just on the measurement time. Other possibilities are the sudden changes caused by placing the electrode into the measurement cell or by removing the electrode from the cell. Without better knowledge, we selected the Cl_{recai} values as the “correct ones” and used them in further interpretations.

The chloride concentrations measured with the ISE are clearly higher than the concentrations determined with the dispersion method, as seen in Figure 13 and Table 5. The effect is stronger in the case of the high density samples, too. A probable explanation is that chloride is excluded from the interlamellar pores and is dissolved only in the non-interlamellar pores where the ISEs measure the concentration. The concentrations calculated on the basis of dispersion analyses assume that the chloride is dissolved in the whole porewater (i.e. IL + non-IL water), which thus gives lower values. The smaller difference between the concentrations at low density is in line with the explanation. At low density, the fraction of the non-IL water increases as seen in Figure 2, leading to a lower concentration with the ISE.

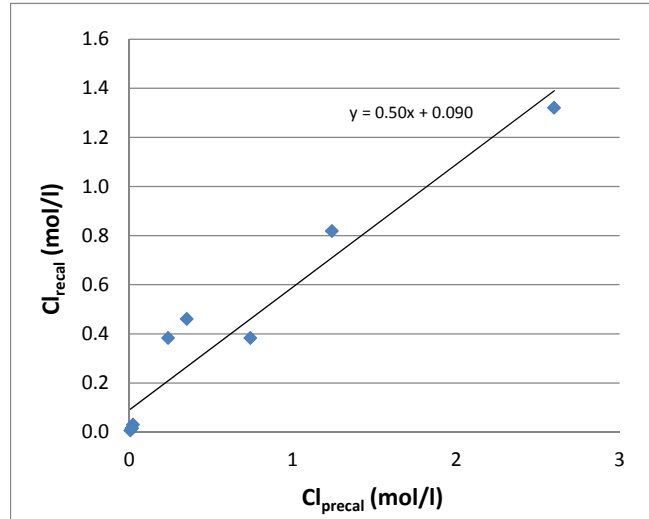


Figure 12. Comparison of the chloride concentration determined with ISEs using the calibration before the experiment (Cl_{precal}) and after the experiment (Cl_{recaI}).

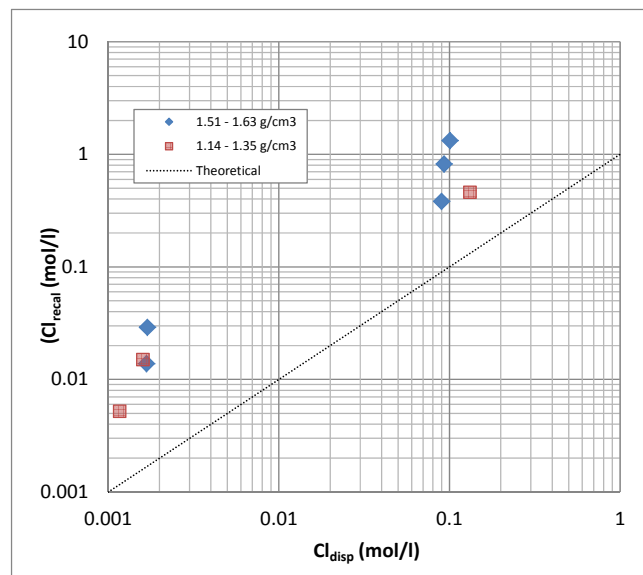


Figure 13. Comparison of the chloride concentrations in bentonite determined with ISE (Cl_{recaI}) and dispersion method (Cl_{disp}). The ISE values are based on the calibration after the experiment. The densities of the bentonite samples are given in the legend.

Figure 14 presents the calcium and chloride concentrations in bentonite determined with the dispersion method. The concentrations are calculated per the total porewater volume. The slope is approximately correct, i.e. the increase of the calcium concentration is about half of the chloride concentration. However, at low chloride concentration the calcium concentration is too high. This is probably caused by some solubility-limited component in the bentonite. In the measurement, the bentonite sample is dispersed into a large volume of deionized water, which allows an excess dissolution of the solubility-limited components. At low concentrations of the added CaCl_2 most of the calcium seems to come from the dissolved component, and the effect is about 20 % even at the highest concentration of the added CaCl_2 . The values determined with the dispersion method are thus not correct in the case of calcium.

Figure 15 compares the calcium and chloride concentrations determined with ISEs in the high-density bentonites. The calcium concentrations are based on the pre-calibration curves and the chloride concentration on the re-calibration curves. The measurement results correlate clearly, but the chloride concentrations are by a factor of three too high. It is obvious that some drift occurs in the calcium electrodes during the measurement. The calcium concentrations based on the re-calibration are clearly erroneous, which indicates that the calibration changes also during the removal of the electrode from the bentonite. In the low-density samples the calcium electrodes give clearly erroneous values, too.

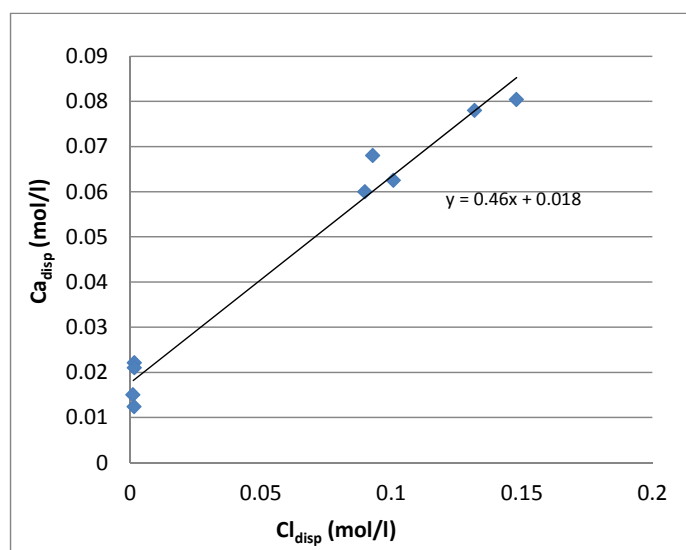


Figure 14. Presentation of the calcium concentrations as a function of chloride concentration in the bentonite. The concentrations were determined with the dispersion method and calculated per the total porewater volume.

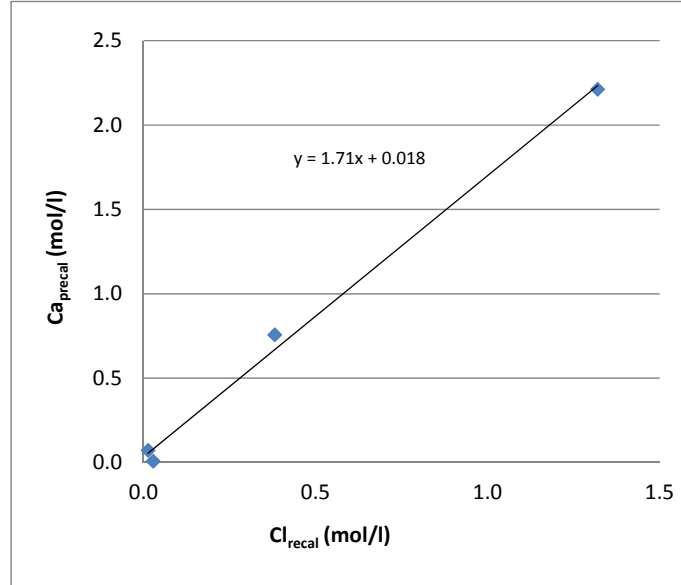


Figure 15. Comparison of the calcium and chloride concentrations determined with ISEs in the high-density bentonites. The calcium concentrations are based on the pre-calibration and chloride concentration on the re-calibration curves.

The chloride porosity values were evaluated on the basis of the ISE measurements and dispersion analyses. The dispersion method gives the chloride concentration in the bentonite sample as mmol/g of dry bentonite. Knowing the concentration given by the ISEs, it is possible from equation (6) to evaluate in which volume of the porewater the chloride has dissolved, i.e. what the chloride porosity is.

$$\varepsilon_{Cl} = \frac{Cl_d \rho_{dry}}{Cl_{ISE}} 100 \quad (6)$$

where ε_{Cl} is the chloride porosity (%), Cl_d is the chloride concentration in bentonite determined with the dispersion method (mmol/g), ρ_{dry} is the dry density of the bentonite (g/cm^3), and Cl_{ISE} is the chloride concentration in the bentonite determined with the ISE (mmol/ml). Figure 16 presents the chloride porosity values determined in this study as a function of the dry density of bentonite together with the values determined in the exclusion experiments in MX-80 and Deponit in Muurinen (2009). The ISE values are shown separately for the samples prepared with the 0.001 M and 0.1 M CaCl_2 solution. The conditions in this study and in Muurinen (2009) are not exactly comparable with each other. In this study, a purified bentonite in calcium form was used. In Muurinen (2009) MX-80 at the beginning of the test had 83 % Na, 2 % K, 9 % Ca and 6 % Mg of the CEC, and in Deponit the values were 24 % Na, 2 % K, 45 % Ca and 29 % Mg. In Figure 16 there is one point which is clearly an outlier; otherwise the measured points of this study fit rather well the curves of MX-80 and Deponit. This suggests that the electrodes measure the concentration in the non-IL pores. No clear effect on the porosity is caused by the different CaCl_2 concentrations in the bentonites, which may indicate a low thickness of the double layers in the calcium bentonite.

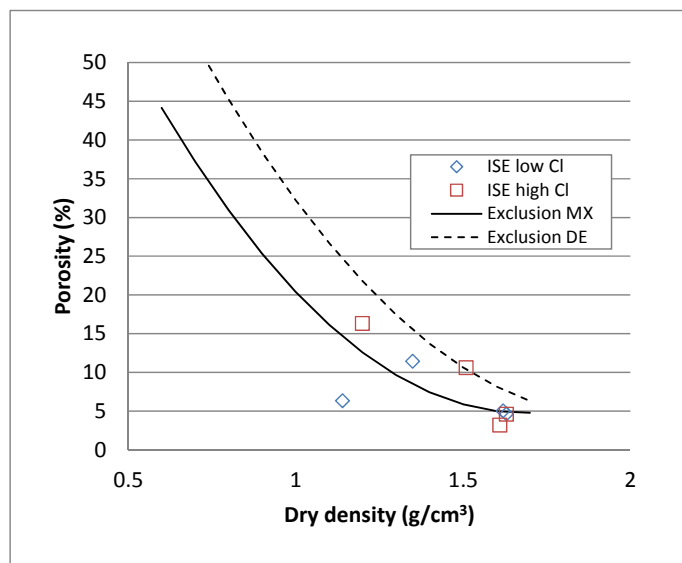


Figure 16. Chloride porosity based on the ISE and dispersion measurements of this study and exclusion measurement in MX-80 and Deponit of Muurinen (2009).

4.3.3 Results of sulphate and sodium electrodes

The results obtained with the sulphate and sodium electrodes in the different bentonite samples are presented in Figures B1 – B4 in Appendix B. Each figure gives the results of one bentonite sample. The uppermost figure (a) presents the measured potentials of the sodium and sulphate electrode as a function of time for each sample. The figures (b) and (c) present the calibration curves of the sodium and sulphate electrodes before and after the experiment and the measured potential in the bentonite at the end of the measurement. The crossing points of the measured potential line with the calibration curves give the logarithms of the measured concentrations in bentonite on the x-axis. The potential curves of sulphate and sodium in Appendix B stabilize typically in a week and stay rather constant through the measurement. The calibration curves of sodium and sulphate before and after the experiment are in many cases far from each other. In some cases the measured potential is clearly out of the calibration area (see Na-1 in Figure B1 and S-2 in Figure B2) and it is questionable if the electrodes have worked properly in such a case.

Table 6 presents the concentrations of sodium and sulphate in the bentonite samples determined with the dispersion method. In the calculations the porewater density was assumed to be 1 g/ml. In the case of sodium and sulphate the interpretation of the measured result is more difficult than in the case of chloride. Although the bentonite was purified before the experiment, it is possible that sulphate comes partly from the dissolution of the solid components. If the dissolution brings also, for example, calcium into the dispersion it can release sodium from the montmorillonite and also the sodium concentration increases. As seen in Table 6, the sulphate concentrations of the low-concentration samples (N3, N4) calculated per the total porewater are clearly higher than the added concentration. Also the sodium concentration is too high compared to the sulphate concentration, which indicates a release by ion exchange from the bentonite. In the case of the high-concentration samples N1 and N2, the sulphate values

are approximately correct but the sodium concentrations are somewhat too high. In Figures B1 and B2 a curve of the “correct calibration” has also been added into the sulphate calibration figure. This curve is obtained such that the sulphate amount determined by the dispersion method is assumed to be approximately correct in the samples N1 and N2 where 0.1 M Na₂SO₄ was mixed as the porewater. This sulphate is dissolved in the porosity of 15 % in the case of N1 and in the porosity of 5 % in the case of N2, according to Figure 16. Calibration curves are then solved which would give those concentrations. In the case of the samples N3 and N4 the same method is not possible because other sources than the added solution bring too much sulphate into the porewater.

The concentrations determined with the electrodes are compared in Table 7 with the sulphate and sodium concentrations which were added into the bentonite when the samples were prepared. Although some increase of the ions can be expected, the added concentrations give probably a good estimation of the average concentration in the whole porewater. It is obvious that the concentrations determined with the ion-selective electrodes are very scattered and unreliable.

Table 6. Sulphate and sodium concentrations in sodium bentonite samples N1 – N4 based on the dispersion measurements.

		N1	N2	N3	N4
Weight of wet bentonite sample	g	2.431	2.088	2.097	2.097
Volume of porewater in the sample	ml	0.776	0.401	0.661	0.413
SO ₄ concentration in dispersion water	mmol/l	3.04	1.85	0.30	0.39
Total SO ₄ in dispersion water	mmol	0.064	0.038	0.006	0.008
SO ₄ concentration per porewater	mol/l	0.083	0.095	0.010	0.020
SO ₄ concentration per dry bentonite	mmol/g	0.039	0.023	0.004	0.005
Na concentration in dispersion water	mmol/l	7.40	5.66	2.70	3.22
Total Na in dispersion water	mmol	0.16	0.12	0.056	0.066
Na concentration per porewater	mol/l	0.20	0.29	0.085	0.16
Na concentration per dry bentonite	mmol/g	0.094	0.069	0.039	0.039

Table 7. Sulphate and sodium concentrations added in the bentonite during the preparation and determined with ion-selective electrodes (ISE). “Pre-cal” means calibration before the experiment and “re-cal” calibration after the measurement.

Sample code	Dry density (g/cm ³)	SO ₄ conc. of porewater (added) (mol/l)	Na conc. of porewater (added) (mol/l)	SO ₄ _{pre} conc. of porewater (ISE, pre-cal.) (mol/l)	SO ₄ _{re} conc. of porewater (ISE, re-cal.) (mol/l)	Na _{pre} conc. of porewater (ISE, pre-cal.) (mol/l)	Na _{re} conc. of porewater (ISE, re-cal.) (mol/l)
N1	1.20	0.1	0.2	1.00E-06	0.037	2.90E-04	0.00
N2	1.66	0.1	0.2	13	15	0.025	1.09
N3	1.21	0.001	0.002	1.07	0.065	36	0.001
N4	1.64	0.001	0.002	0.795	0.021	140	0.32

5 SUMMARY AND DISCUSSION

The aim of this study was to develop and test ion-selective electrodes for measuring the chemical conditions in the porewater of compacted bentonite. The conditions in the porewater of compacted bentonite differ from those in soft clay. Most of the water in compacted bentonite is chemically bound for hydration of the exchangeable cations in the narrow interlamellar spaces of the montmorillonite. Only a part of the pores are so large that the water can be considered as free. It is usually assumed that the amount of water involved in the geochemical processes in the bentonite corresponds to the water in the large non-interlamellar pores, while free ions are strongly excluded from the interlamellar space. The exchangeable cations of the interlamellar space participate in the development of the porewater chemistry by diffusion and cation-exchange processes, however. Usually the geochemical porosity is supposed to be equivalent to the accessible porosity to chloride. The amount of that porosity depends then on the dry density and salinity in the system. At the dry density planned to be used for buffer in the disposal of nuclear wastes ($> 1.5 \text{ Mg/m}^3$), the external porosity is assumed to be a few per cent in freshwater conditions and can increase up to 10 % in saline groundwater conditions where the double layers are thin.

Ion-selective electrodes (ISE) are sensors that convert the chemical activity of an ion in a solution into an electrical potential. The potential is theoretically dependent on the logarithm of the chemical activity of the ion according to the Nernst equation. Compacted bentonite sets special requirements for the ISEs used in the measurements. The high swelling pressure, which can rise to several MPa, can break the electrode or change the properties of the ion-selective membrane. The content of the solid material can rise at the planned buffer density to 55 – 60 volume% such that the membrane is in contact with both the solid material and the porewater. Most of the porewater is, however, interlamellar, which cannot be in direct contact with the electrode. The measurement times have to be rather long, in many cases weeks or months, and the electrodes cannot be calibrated during the measurement, which sets requirements on the potential stability.

The most abundant ions in bentonite for which electrodes should be found are Na^+ , Ca^{2+} , Mg^{2+} , Cl^- , SO_4^{2-} and HCO_3^- . The earlier experiences with an IrOx electrode for pH measurement and some pre-tests with Ag/AgCl and polymer-type electrodes suggested that the inorganic precipitate-type electrodes could withstand better the condition in the compacted bentonite. The focus of the study was then directed to the electrodes of the precipitate-type membranes. From the literature, promising electrode types were found for chloride, sulphate, sodium and calcium. No suitable precipitate-type electrode was found from the literature for HCO_3^- .

The electrode body in which the ion-selective membranes were fixed was constructed from a PEEK screw (M8) aimed to be fixed into the measurement cell used in the bentonite measurements. The chloride electrodes were based on the commercial Ag-AgCl pellets prepared from a fine-grain homogeneous mixture of silver and silver chloride. The pellet was fixed with epoxy in the electrode body. The membrane pellets for the sulphate electrodes were based on a four-component mixture of PbSO_4 , PbS , Ag_2S and Cu_2S pressed overnight at 7 000 bar at 150 °C. Nasicon (Natrium Super Ionic Conductor) was used as a membrane for the sodium electrodes. The Nasicon powder

was pressed for two hours at 4 000 bar at 200 °C and the pellet was sintered in an oven at 1 000 °C. Commercially available europium-doped LaF₃ pellets coated with colloidal CaF₂ and heated to 400 °C were used as the membrane of the calcium electrodes. In the sulphate, sodium and calcium electrodes, the electrical contact between the membrane and the silver wire in the electrode was made with silver epoxy.

The dissolving components of natural bentonite can create complex chemical conditions in the porewater. In order to avoid the problem, the bentonites aimed for the electrode tests were purified by trying to remove the easily dissolving components like gypsum and chlorides and by changing the montmorillonite to sodium or calcium form. The compacted samples for the measurements with the ion-selective electrodes were prepared from the purified clays in squeezing cells. In the case of the sodium bentonite, Na₂SO₄ solutions were added to the bentonite, and sodium and sulphate concentrations were the measured ions. In the case of calcium bentonite, CaCl₂ solutions were added to the bentonite, and calcium and chloride concentrations were the measured ions. The calibrations of the electrodes were done in Na₂SO₄ and CaCl₂ solutions before and after the measurements in the bentonite. The leak-free electrode LF-2 of Innovative Instruments, Inc., Tampa, USA, was used as the reference electrode. The electrode is based on the Ag/AgCl wire in 3.4 M KCl solution and uses a leak-free conductive junction. The electrode body is constructed from PEEK.

The potential measurements in the bentonite were continued for a few weeks. The concentration in the porewater was calculated from the measured potential and the calibration curves.

The potential curves of chloride stabilized typically in one to two days and remained constant through the measurement. The calibration curves before and after the experiment were close to each other, too. The chloride concentrations measured with the ISE were clearly higher than the concentrations assuming a homogeneous distribution in the porewater. The effect was stronger in the case of the high-density samples. The chloride porosities evaluated on the basis of the ISE measurements were in line with the chloride porosities determined earlier in exclusion experiments. The probable explanation is that chloride is excluded from the interlamellar pores and stays in the non-interlamellar pores where the ISEs measure the concentration.

The potentials of the calcium electrodes stabilized much more slowly than the chloride electrodes, and in many cases changing continued through the measurement. The calibration curves of the calcium electrodes before and after the experiment were in many cases far from each other. The calcium concentrations based on the pre-calibration curves and the chloride concentration based on the re-calibration curves correlate clearly, but the calcium concentrations were by a factor of three too high. It is obvious that some drift occurs in the calcium electrodes during the measurement. The calcium concentrations based on the re-calibration were clearly erroneous, which indicated that the calibration changed also during the removal of the electrode from the bentonite.

The potential curves of sulphate and sodium stabilized typically in a week and stayed rather constant through the measurement. The calibration curves of sodium and sulphate before and after the experiment were in many cases far from each other. It is obvious

that the concentrations determined with the ion-selective electrodes of sulphate and sodium were very scattered and unreliable.

Mechanically all the electrodes were strong enough for the measurements in the compacted bentonite, but the stability was a problem in many cases. A possible reason which could cause the insufficient stability and reproducibility of the sodium, calcium and sulphate electrodes is the solid contact between the membrane and the metal wire. In principle, there are different points during the measurement where the electrode can change its properties. The drift can be continuous and depend just on the measurement time. Other possibilities are a sudden change caused by placing the electrode into the measurement cell or by removing the electrode from the cell. The best results were obtained with the chloride electrodes. The change of calibration curves of the chloride electrodes was small both in the solution and bentonite measurements. The results with the calcium electrodes were somewhat promising but the fixing of the CaF_2 coating on the LaF_3 pellet is not strong enough and a better method should be found. CaF_2 should be part of the $\text{La}(\text{Eu})\text{F}_3$ crystal. In the case of the sodium and sulphate electrodes, the drift was strong both in solution and in bentonite, and the electrodes did not work properly. In the case of the sodium electrode, sodium molybdenum bronze ($\text{Na}_x\text{Mo}_6\text{O}_{17}$) could offer an alternative membrane material. The polymer-based membranes would offer an alternative solution for all the ions if the strength and stability of the membrane can be improved markedly.

REFERENCES

Angst, U., Vennesland, 2009. Ø. Detecting critical chloride content in concrete using embedded ion selective electrodes – effect of liquid junction and membrane potentials. *Materials and Corrosion*, vol. 60, pp. 638 – 643.

Bakker, E., Bühlmann, P., Pretsch, E. 1997. Carrier-based ion-selective electrodes and bulk optodes. 1. General Characteristics. *Chem. Rev.*, vol. 97, 3083 – 3132.

Bakker E. 2004. Electrochemical sensors. *Anal Chem.*, vol. 76, 3285 – 3298.

Birgersson, M. & Karnland, O. 2009. Ion equilibrium between montmorillonite interlamellar space and the external solution. *Geochimica and Cosmochimica Acta*, 73, 1908 – 1923.

Bobacka, J., Ivaska, A., Lewenstam, A. 2008. Potentiometric ion sensors. *Chem. Rev.* vol. 108, 329 – 351.

Bobacka, J. 2006. Conducting polymer-based solid-state ion-selective electrodes. *Electroanalysis*, vol. 18, No. 1, 7 – 18.

Bolt, C.F. and Warkentin, B.P. 1958. The negative adsorption of anions from clay suspensions. *Kolloid-Zeitschrift*, Vol. 156, pp. 41-46.

Bradbury, M. H., Baeyens, B. 2002. Porewater chemistry in compacted re-saturated MX-80 bentonite: Physico-chemical characterisation and geochemical modelling. *PSI Bericht Nr. 02-10*.

Bolt, G. & De Haan, F. 1982. *Soil Chemistry B. Physico-Chemical Models*. Elsevier, Amsterdam/New York.

Bradbury, M.H. & Baeyens, B. 2003. Porewater chemistry in compacted re-saturated MX-80 bentonite. *Journal of Contaminant Hydrology*, 61, 329-338.

Bruno, J., Arcos, D., Duro, L. 1999. Processes and features affecting the near field hydrochemistry. Groundwater-bentonite interaction. *SKB Technical Report TR-99-29*.

Bühlmann, P., Pretsch, E., Bakker, E. 1998. Carrier-based ion-selective electrodes and bulk optodes. 2. Ionophores for potentiometric and optical sensors. *Chem. Rev.*, vol. 98, 1593 – 1687.

Caneiro, A., Fabry, P., Khireddine, H., Siebert, E. 1991. Performance characteristics of sodium super ionic conductor prepared by the sol-gel route for sodium ion sensors. *Anal. Chem.*, vol. 63, 2550 – 2557.

Carlsson, T., Muurinen, A., Matuszewicz, M., Root, A. 2012. Porewater in compacted water-saturated bentonite. *Mater. Res. Soc. Symp. Proc. Vol 1475*. Materials Research Society. DOI: 10.1557/opl.2012

Colomban, Ph. 1989. Gel technology in ceramics, glass-ceramics and ceramic-ceramic composites

Crespo, G., Macho, S., Rius, F. 2008. Ion-selective electrodes using carbon nanotubes as ion-to-electron transducers. *Anal. Chem.*, vol. 80, pp. 1316 – 1332.

Curti, E. 1993. Modelling Bentonite Pore Waters for the Swiss High-level Radioactive Waste Repository. Helsinki: Wettingen, Switzerland, NAGRA, 74 p. + app. 11 p. (NTB 93-45).

Curti, E., Wersin, P. 2002. Assessment of porewater chemistry in the bentonite backfill for the Swiss SF/HLW repository. NAGRA Technical Report 02-09. Nagra, Wettingen, Switzerland.

de Haan, F.A.M. 1964. The negative adsorption of anions (anion exclusion) in systems with interacting double layers. *Journal of Physical Chemistry*. Vol. 68, pp. 2970 - 2977.

Domènech, C., Arcos, D., Bruno, J., Karnland, O., Muurinen, A. 2004. Geochemical model of the granite-bentonite-groundwater at Äspö (LOT experiment). *Mat. Res. Soc. Symp. Proc.*, Vol. 807, pp. 855-860.

Edwards, D.C. and Quirk, J.P. 1962. Repulsion of chloride by montmorillonite. *J. Coll. Sci.* Vol. 19, pp. 872 - 882.

Eriksen, T. & Jacobsson, A. 1984. Diffusion in clay. Experimental techniques and theoretical models. Swedish Nuclear and Fuel Supply Co., Stockholm. KBS Technical Report 84 – 05.

Farren, G. 1972. Ion selective electrode for activity determination of cations which do not form as ionic semiconductors. United States Patent 3,657,093.

Fernández, A. M., Baeyens, B., Bradbury, M., Rivas, P. 2004. Analysis of the porewater chemical composition of a Spanish compacted bentonite used in an engineered barrier. *Physical Chemistry of the Earth* 29, 105-118.

García-Sineriz, J., Fuentes-Cantilla, J. 1999. On-line measurement of quality parameters of bentonite based drilling muds. *Automation and Robotics in Construction XVI*, pp. 673 – 677.

Haber, F., Klemensiewicz, H. 1909. Über elektrische Phasengrenzkraft. *Zeitschrift für Physicalische Chemie*, vol. 67, p. 385.

Ivanova N.M., Levin, M.B., Mikhelson, K.N. 2012. Problem and prospects of solid contact ion-selective electrodes with ionophore-based membranes. *Russian Chemical Bulletin, International Edition*, vol. 61, pp. 926 – 936.

Janata, J. 2009. Principles of chemical sensors, 2nd ed. Springer Science+Business Media, New York.

Jaworska, E., Wóciak, M., Kisiel, A., Mieczkowski, J., Michalska, A. 2011. Gold nanoparticles solid contact for ion-selective electrodes of highly stable potential readings. *Talanta*, vol. 85, pp. 1986 – 1989.

Juvankoski, M., 2010. Description of basic design for buffer. Posiva Working Report 2009-131.

Karnland, O., Olsson, S., Nilsson, U. 2006. Mineralogy and sealing properties of various bentonites and smectite-rich clay materials. SKB, Stockholm, Sweden. SKB Technical Report TR-06-30.

Kolthoff, I.M., Sanders, H.L. 1937. Electric potentials at crystal surfaces, and silver halide surfaces in particular. *Journal of American Chemical Society*, vol 59, 416 – 420.

Kozaki, T. Inada, K., Sato, S. & Ohashi, H. 2001. Diffusion mechanisms of chloride in sodium montmorillonite. *Journal of Contaminant Hydrology* 47,159 – 170.

Luukkonen, A. 2004. Modelling Approach for Geochemical Changes in the Prototype Repository Engineered Barrier System. Posiva Working Report 2004-31.

Melamed, A., Pitkänen, P., Olin, M., Muurinen, A. and Snellman, M. 1992. Interaction of water and compacted sodium bentonite in simulated nuclear waste disposal conditions. In: Sombret, C. G. (ed.) *Materials Research Society. Symp. Proc.*, vol. 257. (Scientific Basis for Nuclear Waste Management XV). Pittsburgh, Pennsylvania: Materials Research Society. Pp. 557 - 566. ISBN 1-558899-151-4

Mohan, M.S., Rechnitz, G.A. 1973. Preparation and properties of sulphate ion selective membrane electrode. *Analytical Chemistry*, vol. 45, 1323 – 1326.

Moleira, M., Eriksen, T. & Jansson, M., 2003. Anion diffusion pathways in bentonite clay compacted to different dry densities. *Applied Clay Science* 23, 69 – 76.

Montavon, G., Guo, Z., Tournassat, C., Grambow, B. & Le Botlan, D. 2009. Porosities accessible to HTO and iodide on water-saturated compacted clay materials and relation with the forms of water: A low field proton NMR study. *Geochimica et Cosmochimica Acta*, 73, 7290-7302.

Muurinen, A. 1994. Diffusion of anions and cations in compacted sodium bentonite. Espoo: Technical Research Centre of Finland, VTT Publications 168.

Muurinen, A., Aalto, H., Carlsson, T., Lehtikoinen, J., Melamed, A., Olin, M., and Salonen, P. 1995. Interaction of fresh and saline waters with compacted bentonite. Espoo: Technical Research Centre of Finland. 29 p. + app. 14 p. (VTT Research Notes 1714). ISBN 951-38-4869-8

- Muurinen, A., Lehtikoinen, J., Melamed, A., and Pitkänen, P. 1996. Chemical interaction of fresh and saline waters with compacted bentonite. Espoo: Technical Research Centre of Finland. 26 p. + app. 3 p. (VTT Research Notes 1806). ISBN 951-38-5081-1
- Muurinen, A., Lehtikoinen, J. 1999. Porewater Chemistry in compacted bentonite. Report Posiva 99-20.
- Muurinen, A., Carlsson, T. 2007. Development of methods for on-line measurements of chemical conditions in compacted bentonite. *Physics and Chemistry of the Earth*, vol. 32, pp. 241 – 246.
- Muurinen, A. 2009. Studies on the Chemical Conditions and Microstructure in the Reference Bentonites of Alternative Buffer Materials Project (ABM) in Äspö. Posiva Oy, Olkiluoto. Working Report 2009-42.
- Muurinen, A., Carlsson, T. 2010. Experiences of pH and Eh measurements in compacted MX-80 bentonite. *Applied Clay Science*, vol. 47, pp. 23 – 27.
- Muurinen, A., Carlsson, T. 2013. Bentonite pore structure based on SAXS, chloride exclusion and NMR studies. POSIVA 2013-xx. (To be published).
- Newman A.C.D., Brown G. 1987. *The Chemical Constitution of Clays*, Mineralogical Society. Monograph No.6, ed. A.C.D. Newman, 1987.
- Oesch, U., Ammann, D., Simon, W. 1986. Ion-selective membrane electrodes for clinical use. *Clinical Chemistry*, vol. 32, No. 8, 1448 – 1459.
- Ohe, T., Tsukamoto, M. 1997. Geochemical properties of bentonite pore water in high-level-waste repository condition. *Nuclear Technology*. Vol. 118, pp. 49-57.
- Ohkubo, T., Kikuchi, H. & Yamaguchi, M. 2008. An approach of NMR relaxometry for understanding water in saturated compacted bentonite. *Physics and Chemistry of the Earth*, S169-S176.
- Posiva 2010. TKS-2009. Nuclear waste management at Olkiluoto and Loviisa power plants Review of current status and future plans for 2010-2012. Posiva Oy, Eurajoki.
- Pungor, E. 1997. Ion-selective electrodes – history and conclusions. *Fresenius Journal of Analytical Chemistry*, vol. 357, pp. 184 – 188.
- Pungor, E., Toth, K. 1973. Precipitate-based ion-selective electrodes. *Pure and Applied Chemistry*, vol. 34, No. 1, pp. 105 – 137.
- Salles, F., Douillard, J-M., Denoyel, R., Bildstein, O., Jullien, M., Beurroies, I. & Van Damme, H. 2009. Hydration sequence of swelling clays: Evolutions of specific surface area and hydration energy. *Journal of Colloid and Interface Science* 333, 510 – 522.

Sasaki, Y., Shibata, M., Yui, M., Ishikawa, H. 1995. Experimental studies on interaction of groundwater with bentonite. In: Murakami, T. And Ewing, R.C. (eds.) Materials Research Society. Symp. Proc., vol. 353. (Scientific Basis for Nuclear Waste Management XVIII). Pittsburgh, Pennsylvania: Materials Research Society. Pp. 337 - 344. ISBN 1-55899-253-7

Shuk, P., Greenplatt, M., Ramanujachary, K.V. 1996. Sodium ion sensitive electrode based on a molybdenum oxide bronze. *Solid State Ionics.*, vol. 91, 233 – 238.

Snellman, M., Uotila, H., Rantanen, J. 1987. Laboratory and modelling studies of sodium bentonite groundwater interaction. In: Bates, J.K., Seefeldt, W.B. (eds.). Symp. Proc., vol. 84. Pittsburgh, Pennsylvania: MRS. Pp. 781-790.

Sposito, G. 1982. The diffuse-ion swarm near smectite particles suspended in 1:1 electrolyte solutions: modified Gouy-Chapman theory and quasicrystal formation. In: Clay-water interface and its rheological implications (eds. N. Gyven and R. M. Pollastro). Clay minerals society.

Tahvildari, K., Esmaeilipour, M., Ghammamy, Sh., Nabipour, H. 2012. CaF₂ nanoparticles: Synthesis and characterization. *International Journal of Nano Dimension*, vol. 2, 269 – 273.

Takahashi, M., Muroi, M., Inoue, A., Aoki, M., Takizawa, M., Ishigure, K., Fujita, N. 1987. Properties of bentonite clay as buffer material in high-level waste geological disposal. Part I: Chemical species contained in bentonite. *Nuclear Technology*. Vol. 76, pp. 221-228. ISSN 0029-5450

Tournassat, C. & C.A.J. Appelo. 2011. Modelling approaches for anion-exclusion in compacted Na-bentonite. *Geochimica et Cosmochimica Acta* 75, 3698-3710.

Van Loon, L.R., Glaus, M.A. & Müller, W. 2007. Anion exclusion effects in compacted bentonites: towards a better understanding of anion diffusion. *Applied Geochemistry*, 22, 2536-2552.

van Olphen, H. 1977. Clay colloid chemistry. 2nd ed. New York: John Wiley & Sons. 318 p. ISBN 0-471-01463-X

Wang, F., Huang, P. 1990. Ion-selective electrode determination of solution K in soil suspensions and significance in kinetic studies. *Can. J. Soil. Sci.*, vol. 70, 411 – 425.

Wanner, H. 1987. Modeling interaction of deep groundwaters with bentonite and radionuclide speciation. *Nuclear technology*, Vol. 79, pp. 338-347.

Wersin, P. 2003. Geochemical modelling of bentonite porewater in high-level waste repositories. *Journal of Contaminant Hydrology* 61, 405-422.

Wieland, E., Wanner, H., Albinsson, Y., Wersin, P. and Karnland, O. 1994. A surface chemical model of the bentonite-water interface and its implications for modelling the near field chemistry in a repository for spent fuel. Stockholm, Swedish Nuclear Fuel and Waste Management Co., Report SKB-94-26, 64 p. ISSN 0284-3757.

Zhou, M., Gan, S., Cai, B., Li, F., Ma, W., Han, D., Niu, Li. 2012. Effective solid contact for ion-selective electrodes: Tetrakis(4-chlorophenyl)borate (TB^-) anions doped nanocluster films. *Analytical Chemistry*, vol. 84, pp. 3480 – 3483.

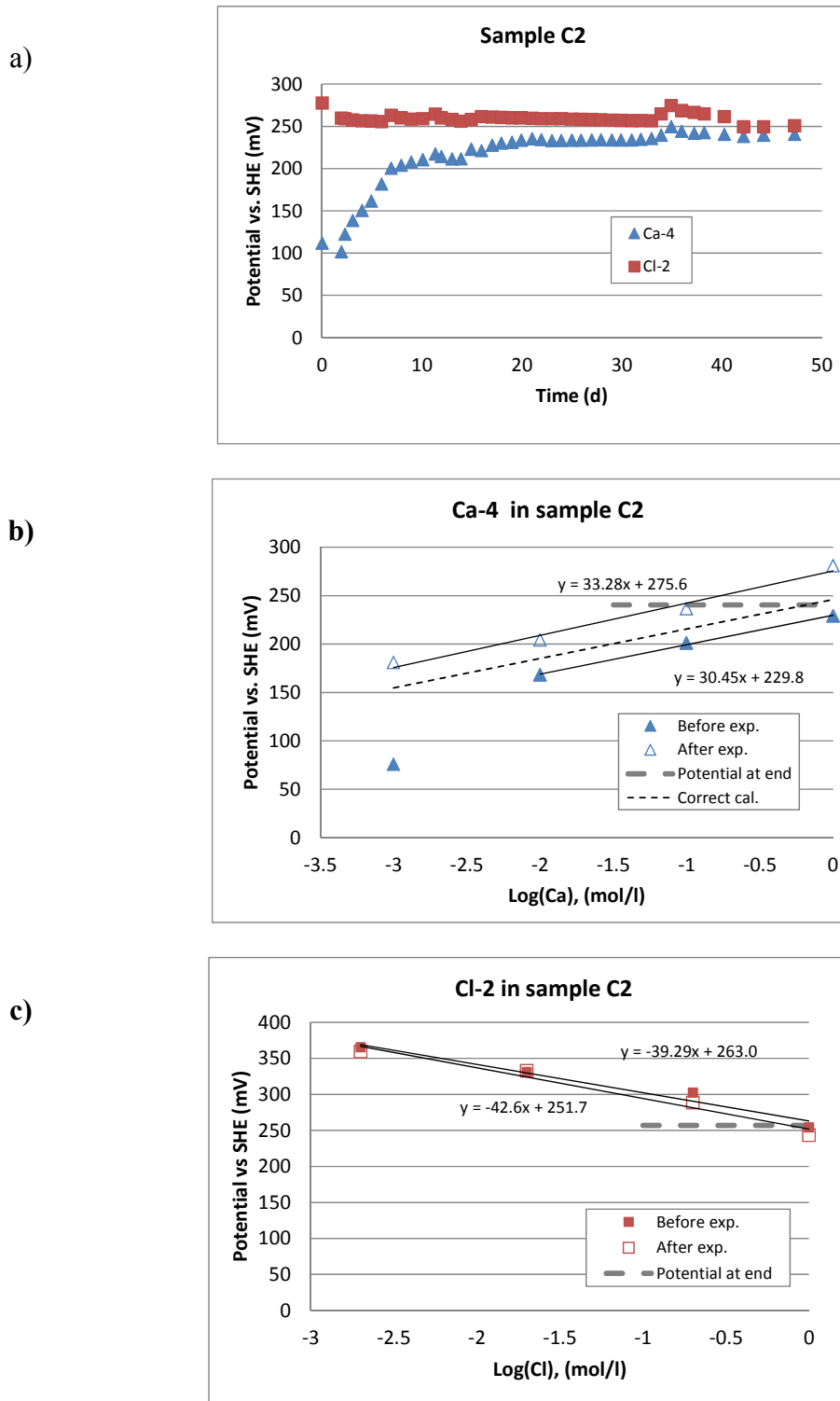


Figure A1. Measurement of calcium and chloride concentrations in the calcium bentonite sample C2. Dry density 1.61 g/cm^3 , measured chloride concentration in bentonite 0.916 mg/g .

a) Measured potentials of Ca-4 and Cl-2 electrodes as a function of time.

b) Calibration of the Ca-4 electrode before and after the experiment and measured potential in bentonite at the end of the measurement. The curve of the correct cal. would give to the calcium half of the chloride concentration.

c) Calibration of the Cl-2 electrode before and after the experiment and measured potential in bentonite at the end of the measurement.

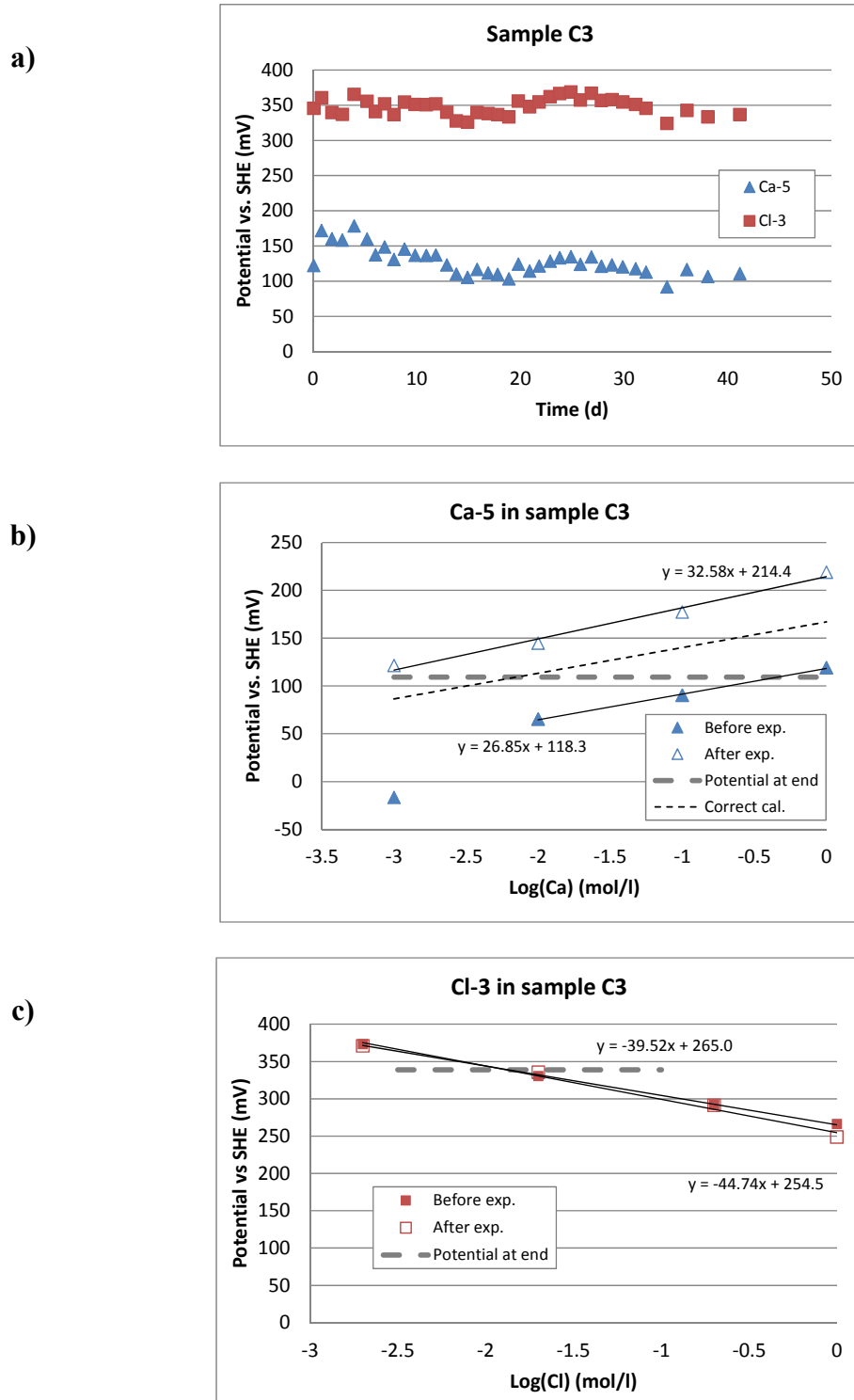


Figure A2. Measurement of calcium and chloride concentrations in the calcium bentonite sample C3. Dry density 1.14 g/cm^3 , measured chloride concentration in bentonite 0.0294 mg/g .

a) Measured potentials of Ca-5 and Cl-3 electrodes as a function of time.

b) Calibration of the Ca-5 electrode before and after the experiment and measured potential in bentonite at the end of the measurement. The curve of the correct cal. would give to the calcium half of the chloride concentration.

c) Calibration of the Cl-3 electrode before and after the experiment and measured potential in bentonite at the end of the measurement.

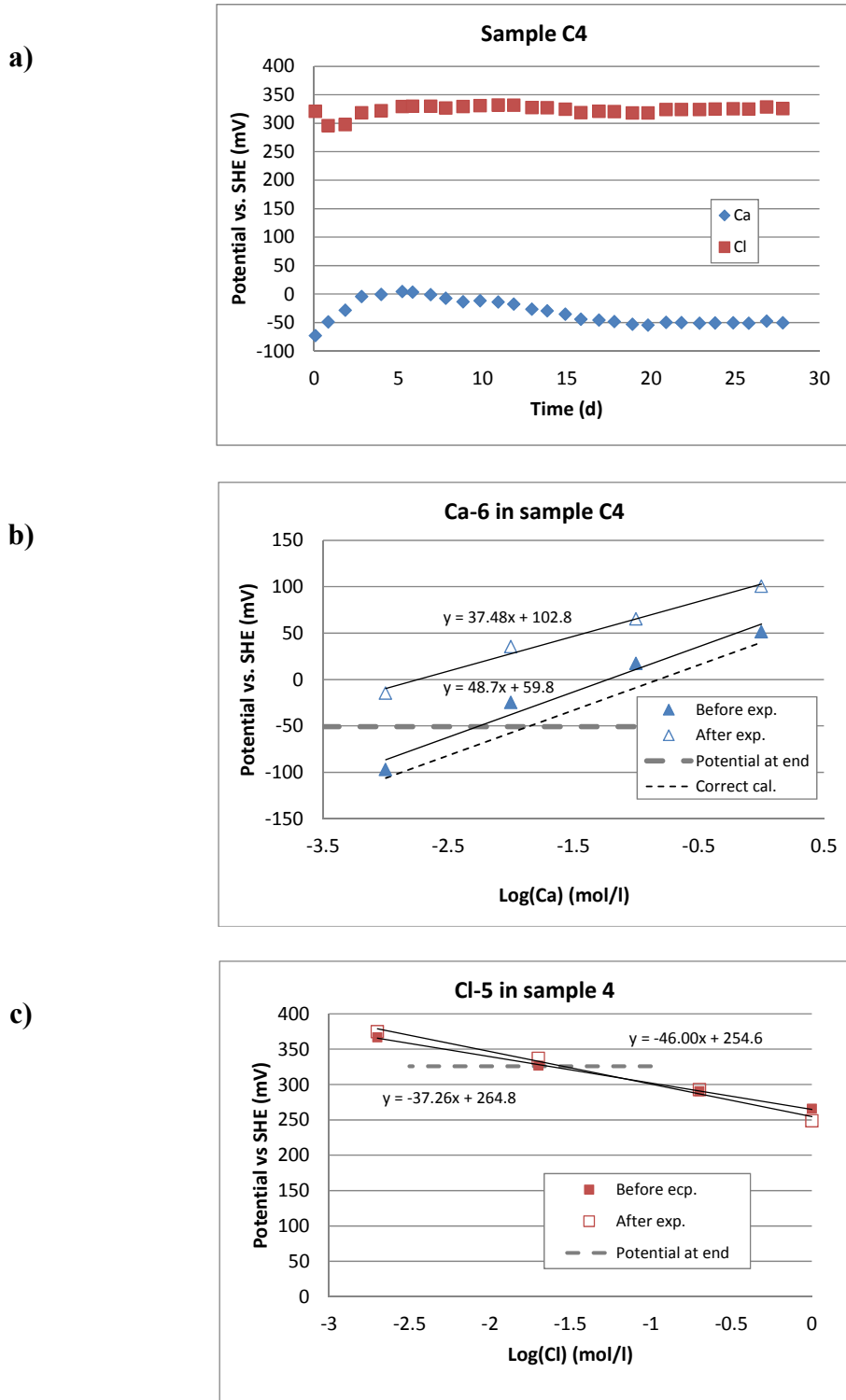


Figure A3. Measurement of calcium and chloride concentrations in the calcium bentonite sample C4. Dry density 1.63 g/cm^3 , measured chloride concentration in bentonite 0.0156 mg/g .

a) Measured potentials of Ca-6 and Cl-5 electrodes as a function of time.

b) Calibration of the Ca-6 electrode before and after the experiment and measured potential in bentonite at the end of the measurement. The curve of the correct cal. would give to the calcium half of the chloride concentration.

c) Calibration of the Cl-5 electrode before and after the experiment and measured potential in bentonite at the end of the measurement.

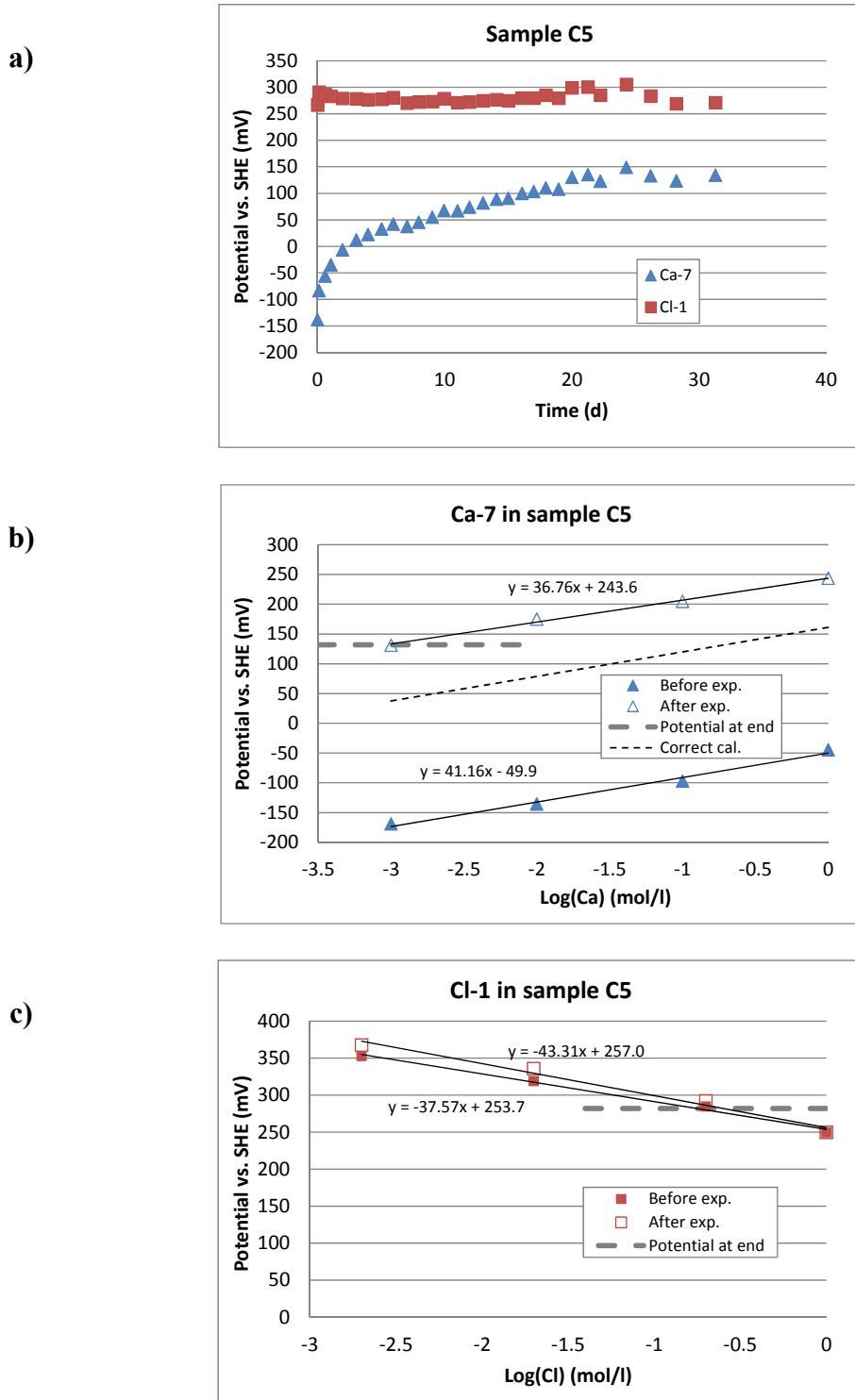


Figure A4. Measurement of calcium and chloride concentrations in the calcium bentonite sample C5. Dry density 1.20 g/cm^3 , measured chloride concentration in bentonite 2.22 mg/g .

a) Measured potentials of Ca-7 and Cl-1 electrodes as a function of time.

b) Calibration of the Ca-7 electrode before and after the experiment and measured potential in bentonite at the end of the measurement. The curve of the correct cal. would give to the calcium half of the chloride concentration.

c) Calibration of the Cl-1 electrode before and after the experiment and measured potential in bentonite at the end of the measurement.

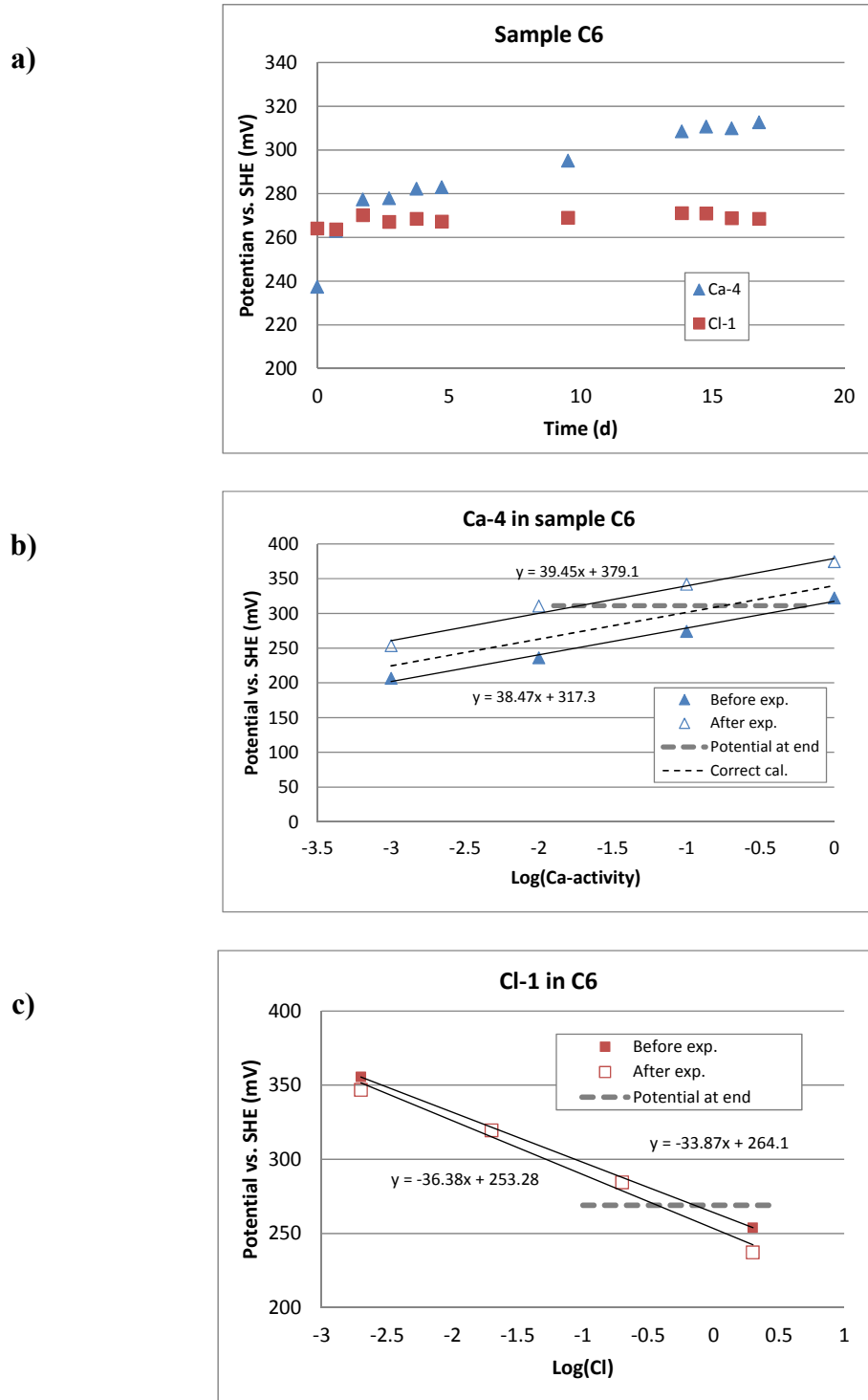


Figure A5. Measurement of calcium and chloride concentrations in the calcium bentonite sample C6. Dry density 1.51 g/cm^3 , measured chloride concentration in bentonite 0.955 mg/g .

a) Measured potentials of Ca-4 and Cl-1 electrodes as a function of time.

b) Calibration of the Ca-4 electrode before and after the experiment and measured potential in bentonite at the end of the measurement. The curve of the correct cal. would give to the calcium half of the chloride concentration.

c) Calibration of the Cl-1 electrode before and after the experiment and measured potential in bentonite at the end of the measurement.

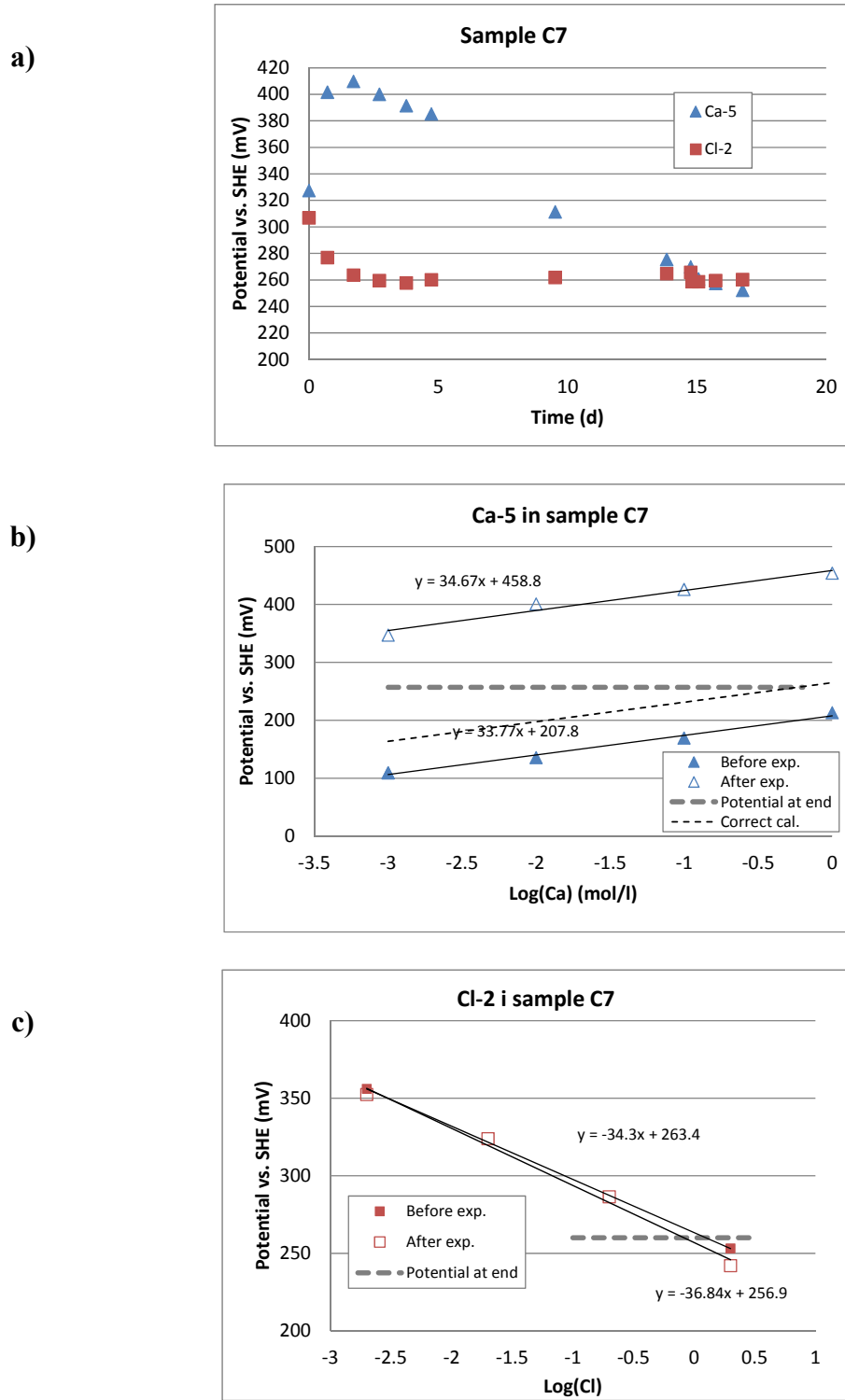


Figure A6. Measurement of calcium and chloride concentrations in the calcium bentonite sample C7. Dry density 1.63 g/cm^3 , measured chloride concentration in bentonite 0.817 mg/g .

a) Measured potentials of Ca-5 and Cl-2 electrodes as a function of time.

b) Calibration of the Ca-5 electrode before and after the experiment and measured potential in bentonite at the end of the measurement. The curve of the correct cal. would give to the calcium half of the chloride concentration.

c) Calibration of the Cl-2 electrode before and after the experiment and measured potential in bentonite at the end of the measurement.

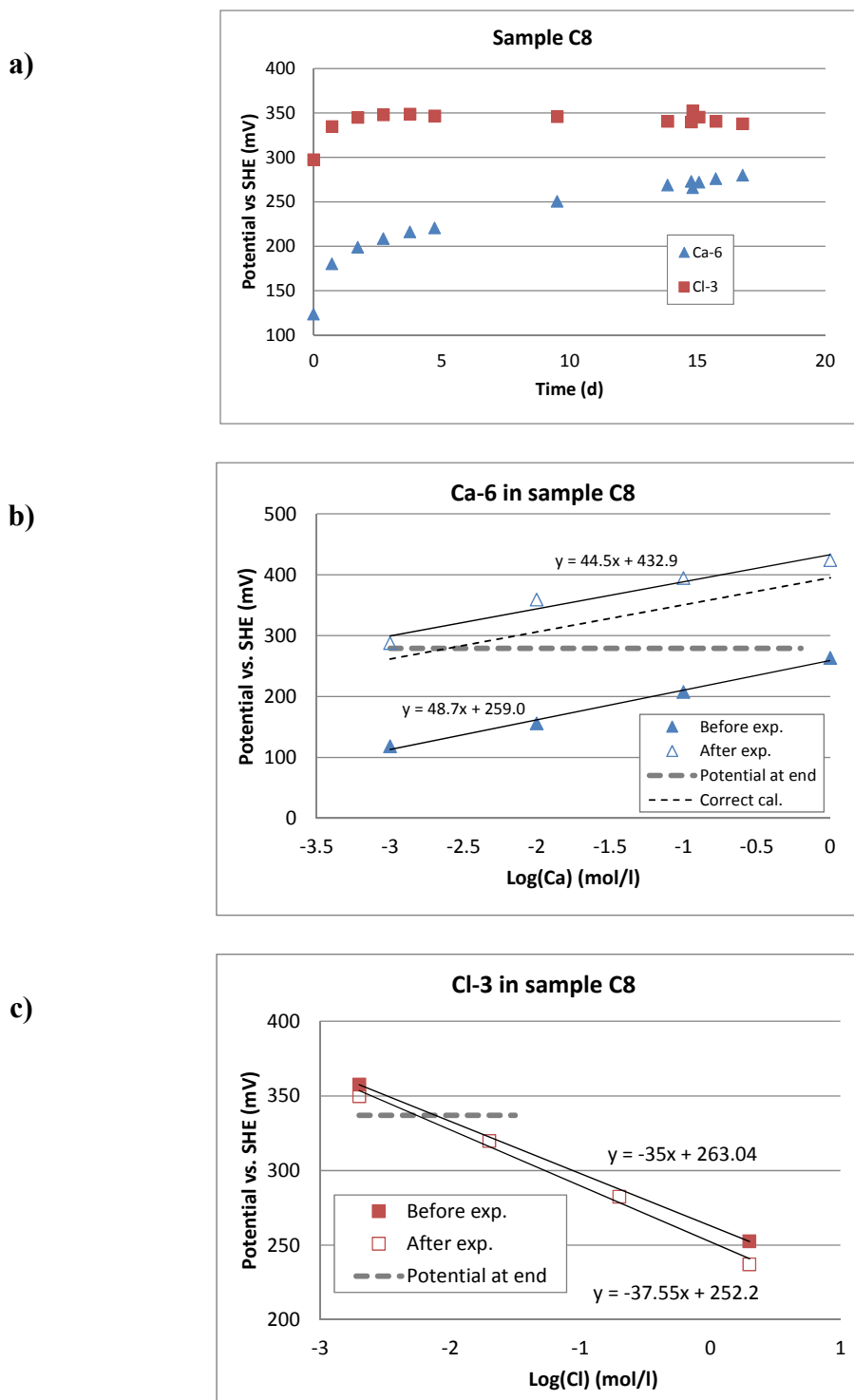
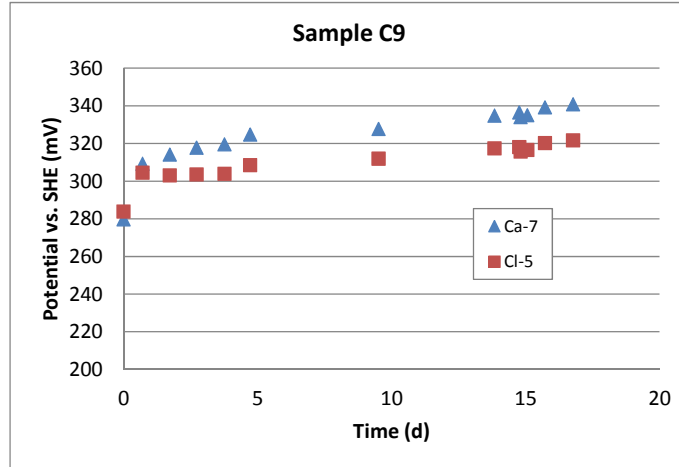


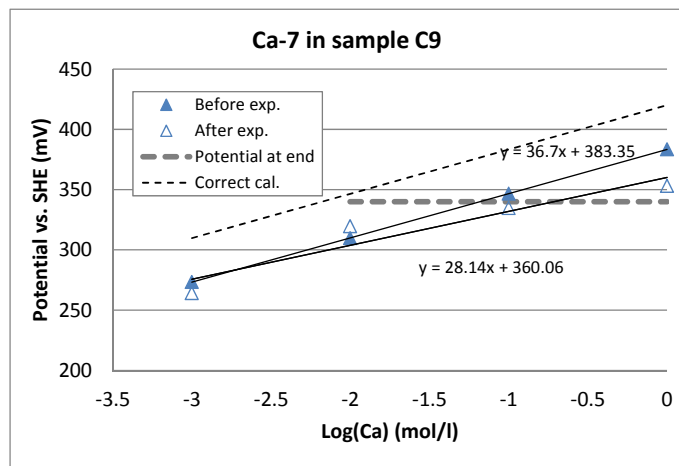
Figure A7. Measurement of calcium and chloride concentrations in the calcium bentonite sample C8. Dry density 1.35 g/cm^3 , measured chloride concentration in bentonite 0.0156 mg/g .

- a) Measured potentials of Ca-6 and Cl-3 electrodes as a function of time.
 b) Calibration of the Ca-6 electrode before and after the experiment and measured potential in bentonite at the end of the measurement. The curve of the correct cal. would give to the calcium half of the chloride concentration.
 c) Calibration of the Cl-3 electrode before and after the experiment and measured potential in bentonite at the end of the measurement.

a)



b)



c)

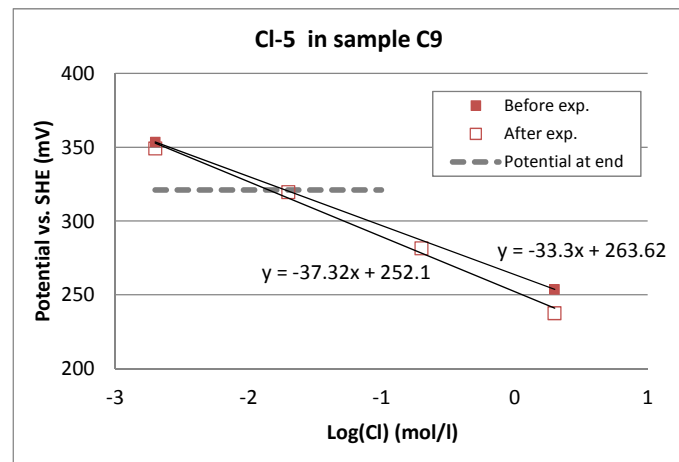


Figure A8. Measurement of calcium and chloride concentrations in the calcium bentonite sample C9. Dry density 1.62 g/cm^3 , measured chloride concentration in bentonite 0.0150 mg/g .

a) Measured potentials of Ca-7 and Cl-5 electrodes as a function of time.

b) Calibration of the Ca-7 electrode before and after the experiment and measured potential in bentonite at the end of the measurement. The curve of the correct cal. would give to the calcium half of the chloride concentration.

c) Calibration of the Cl-5 electrode before and after the experiment and measured potential in bentonite at the end of the measurement.

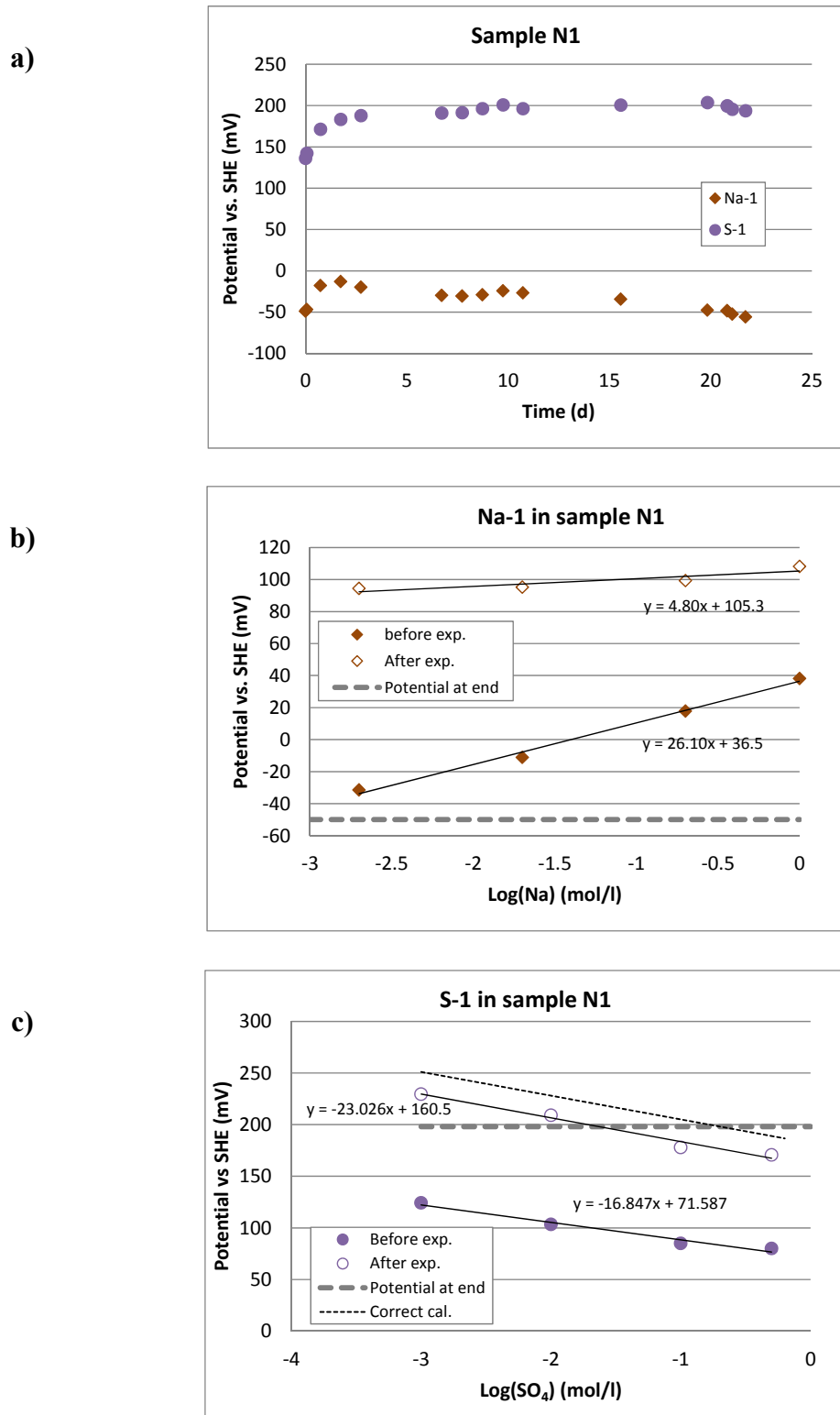


Figure B1. Measurement of sodium and sulphate concentrations in the sodium bentonite sample N1. Dry density 1.20 g/cm^3 .

a) Measured potentials of Na-1 and S-1 electrodes as a function of time.

b) Calibration of the Na-1 electrode before and after the experiment and measured potential in bentonite at the end of the measurement.

c) Calibration of the S-1 electrode before and after the experiment and measured potential in bentonite at the end of the measurement.

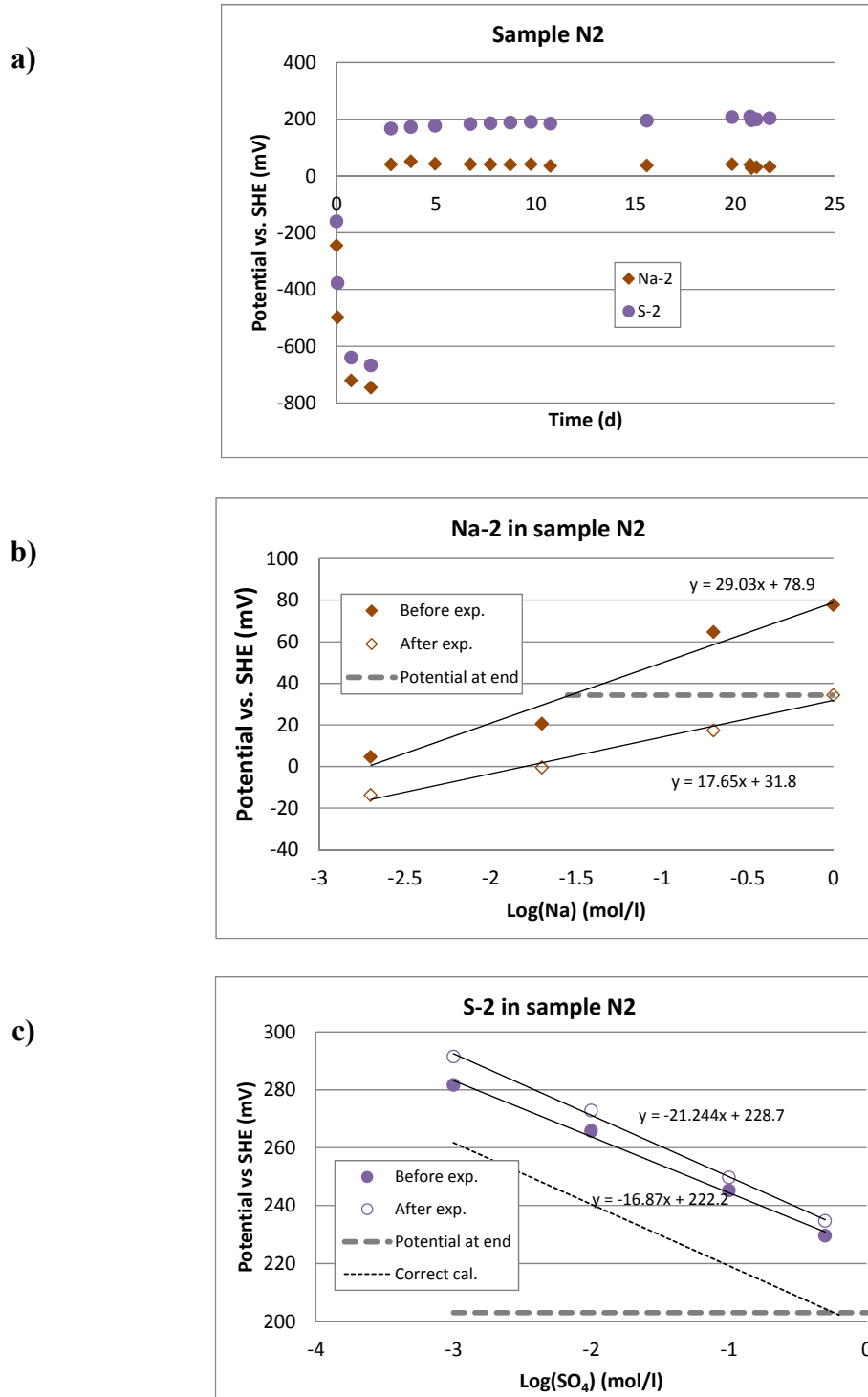


Figure B2. Measurement of sodium and sulphate concentrations in the sodium bentonite sample N2. Dry density 1.66 g/cm^3 .

a) Measured potentials of Na-2 and S-2 electrodes as a function of time.

b) Calibration of the Na-2 electrode before and after the experiment and measured potential in bentonite at the end of the measurement.

c) Calibration of the S-2 electrode before and after the experiment and measured potential in bentonite at the end of the measurement.

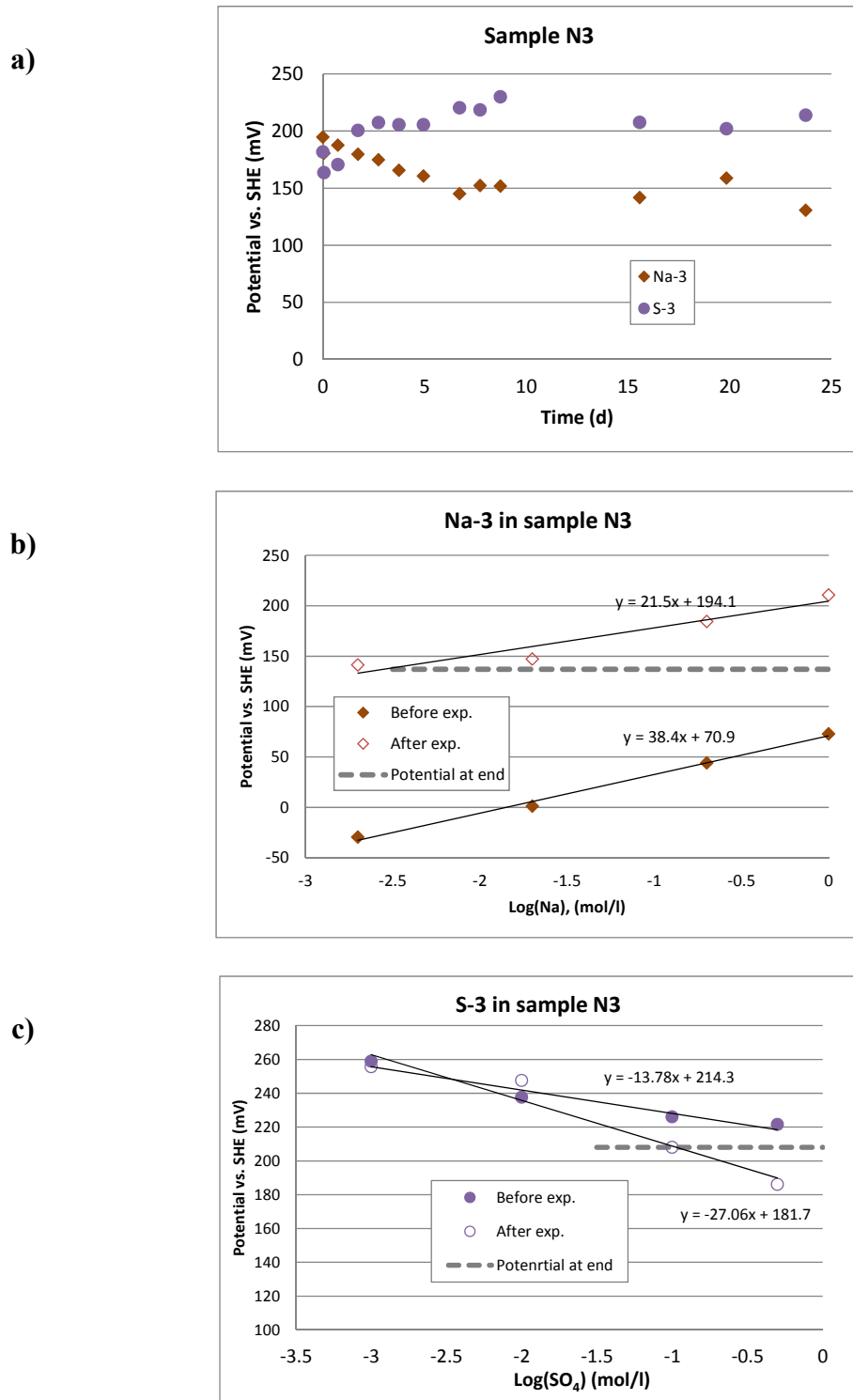


Figure B3. Measurement of sodium and sulphate concentrations in the sodium bentonite sample N3. Dry density 1.21 g/cm^3 .

a) Measured potentials of Na-3 and S-3 electrodes as a function of time.

b) Calibration of the Na-3 electrode before and after the experiment and measured potential in bentonite at the end of the measurement.

c) Calibration of the S-3 electrode before and after the experiment and measured potential in bentonite at the end of the measurement.

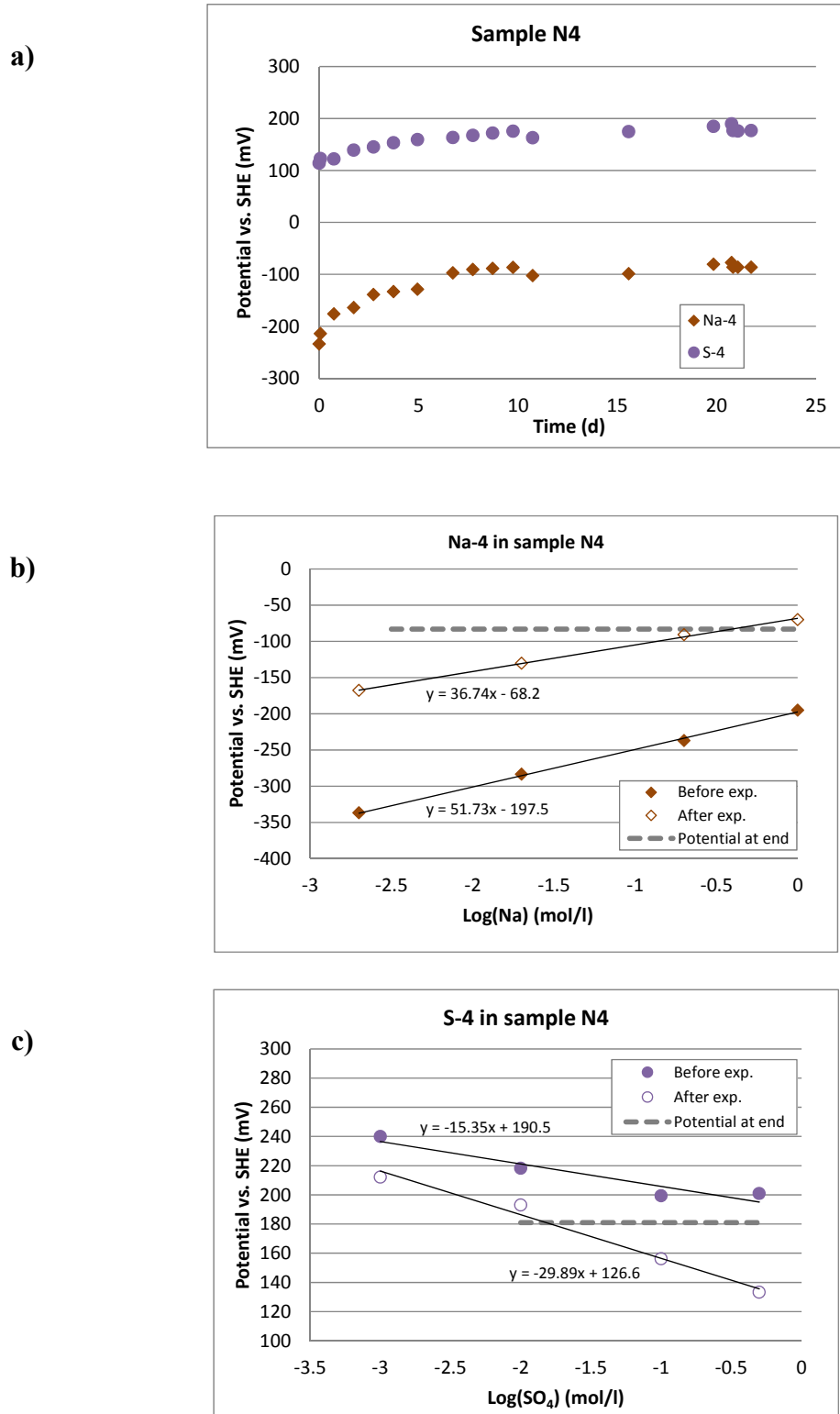


Figure B4. Measurement of sodium and sulphate concentrations in the sodium bentonite sample N4. Dry density 1.64 g/cm^3 .

a) Measured potentials of Na-4 and S-4 electrodes as a function of time.

b) Calibration of the Na-4 electrode before and after the experiment and measured potential in bentonite at the end of the measurement.

c) Calibration of the S-4 electrode before and after the experiment and measured potential in bentonite at the end of the measurement.